

Article

Effectiveness of Immature Asian Pear Extract on Pulmonary Injury Caused by Particulate Matter in Mice

Mi-Ran Kim ^{1,†}, Jin-Hwa Lee ^{1,†}, Mo-Un Ku ², Ki-Young Kim ³, Su Shin ³ , Eun-Jin Hong ³, Sae-Kwang Ku ^{4,*} 
and Jae-Suk Choi ^{1,*} 

- ¹ Department of Seafood Science and Technology, The Institute of Marine Industry, Gyeongsang National University, Tongyeong 53064, Republic of Korea; 210217@gnu.ac.kr (M.-R.K.); evolution_5237@gnu.ac.kr (J.-H.L.)
- ² Department of Biomedical Laboratory Science, College of Health and Welfare, Kyungwoon University, Gumi 39160, Republic of Korea; 202121018@ikw.ac.kr
- ³ Research Institute, Bio Port Korea Inc., Busan 46034, Republic of Korea; kyk1967@bioportkorea.com (K.-Y.K.); sshin@bioportkorea.com (S.S.); ejhong@bioportkorea.com (E.-J.H.)
- ⁴ Department of Anatomy and Histology, College of Korean Medicine, Daegu Haany University, Gyeongsan 38610, Republic of Korea
- * Correspondence: gucci200@dhu.ac.kr (S.-K.K.); jsc1008@gnu.ac.kr (J.-S.C.); Tel.: +82-53-819-1549 (S.-K.K.); +82-55-772-9142 (J.-S.C.)
- † These authors contributed equally to this work.

Abstract: The use of natural products in developing respiratory-function-protective pharmaceuticals is actively progressing. However, in this context, the improvement effects of young Asian pear (*Pyrus pyrifolia* Nakai) extracts have not been evaluated yet. Thus, this study investigated the anti-inflammatory and lung damage improvement effects of immature Asian pear extract (IAP; 400, 200, and 100 mg/kg) using a particulate matter 2.5 μm (PM_{2.5})-induced sub-acute lung injury mouse model. The experimental results were compared with dexamethasone (0.75 mg/kg), used as a control drug. After two intranasal instillations of PM_{2.5} and ten doses of IAP extract for eight days, changes in macroscopic lung autopsy, leukocyte fractionation from bronchoalveolar lavage fluid, lung antioxidant defense system, lung histopathology, and mRNA expression in lung tissue were confirmed. Stress-induced inflammatory lung damage through the increased expression of PM_{2.5}-induced PI3K/Akt and p38 MAPK mRNA was significantly suppressed via the administration of IAP extract (400–100 mg/kg). Furthermore, IAP extract administration promoted serous fluid production in lung tissue, increased substance P and ACh levels, and decreased mucus-production-related expression of MUC5AC and MUC5B mRNA. Interestingly, the observed effects showed a dose-dependent manner without serious hepatotoxicity. The results of this study indicate that a proper oral administration of IAP extract could be helpful in protecting against lung diseases, positioning IAP extract as a potential candidate for an alternative agent to safeguard the respiratory system.

Keywords: Asian pear; *Pyrus pyrifolia*; lung injury; PM_{2.5}; mice; anti-inflammatory activity



Citation: Kim, M.-R.; Lee, J.-H.; Ku, M.-U.; Kim, K.-Y.; Shin, S.; Hong, E.-J.; Ku, S.-K.; Choi, J.-S. Effectiveness of Immature Asian Pear Extract on Pulmonary Injury Caused by Particulate Matter in Mice. *Appl. Sci.* **2023**, *13*, 9578. <https://doi.org/10.3390/app13179578>

Academic Editor: Serge Lavoie

Received: 1 August 2023

Revised: 20 August 2023

Accepted: 22 August 2023

Published: 24 August 2023



Copyright: © 2023 by the authors. Licensee MDPI, Basel, Switzerland. This article is an open access article distributed under the terms and conditions of the Creative Commons Attribution (CC BY) license (<https://creativecommons.org/licenses/by/4.0/>).

1. Introduction

Due to the increase in particulate matter (PM) caused by air pollution, various respiratory diseases are rapidly emerging in East Asia, including China, Korea, and Japan. Beijing, the capital city of China, stands out among these regions, having a notably elevated prevalence of respiratory diseases attributed to PM exposure [1–4]. Efforts to curtail air pollution were intensified when Beijing was spotlighted as one of the most severely impacted cities by PM air pollution during the Beijing Olympics [5]. PM has a diameter of around 2.5 μm (PM_{2.5}) and contains organic contaminants, including polycyclic aromatic hydrocarbons, mineral dust and inorganic contaminants, such as sulfate, nitrate, elemental carbon, and ammonium [6,7].

Inhaling PM can lead to severe lung damage and, subsequently, harm the heart. Asthma is one of the most representative non-communicable respiratory tract diseases caused by air pollution [3,8]. According to the World Health Organization report in 2017 [9], the global prevalence of asthma was estimated to be approximately 235 million people. PM inhalation is recognized as a major cause of allergic inflammation, representing a significant and severe etiological factor in asthma [10]. Over 70% of inhaled PM settles in the lower trachea, while approximately 22% makes its way to the alveoli [11]. The buildup of PM induces oxidative stress in airway and lung tissue's epithelial cells, leading to localized tissue damage, and ultimately triggering inflammatory responses [5,12]. Key factors contributing to oxidative stress in airway epithelial cells include reactive glutathione peroxidase (GPX), reactive oxygen species (ROS), superoxide dismutase (SOD), heme-oxygenase-1 (HO-1), catalase (CAT), and glutathione (GSH) [13]. The initiation of an inflammatory response can easily be measured by an increase in proinflammatory cytokines and inflammatory mediators [14]. Inflammation of the lungs following PM inhalation is caused by an increase in ROS and cytokines (interleukin (IL)-6 and tumor necrosis factor (TNF)- α) in bronchoalveolar lavage fluid (BALF) and the migration of monocytes [1–3,15].

With the increase in respiratory disorders caused by PM, advancements have been made in the development of drugs aimed at treating or preventing respiratory damage [2,3,16]. In particular, natural products produce physiologically active substances with relatively minimal side effects and excellent antioxidant and anti-inflammatory activities [17,18]; thus, the use of PM_{2.5}-induced lung injury models to develop respiratory protection drugs from natural sources is actively progressing [1–3,16,19].

Pears (*Pyrus* spp.) are one of the most purchased fruits globally [20]. Given that pears do not have a distinct color or scent, the study of chemical substances or biological activities present in pears is relatively limited or sparse [21,22]. Based on the existing study on the chemical compounds found in *Pyrus pyrifolia* Nakai [23], an oriental pear most commonly cultivated in Korea, phenylpropanoid malate derivatives [23], caffeoyl triterpenes [24], and flavonoids have been isolated and identified as the major active compounds [25–28]. The main active ingredients in pears, including flavonoids, arbutin, caffeic acid, malaxinic acid, chlorogenic acid, and phenolic compounds, as well as antioxidant activity, decrease with maturation [29], whereas immature pears possess high levels of phenolic compounds and antioxidant activity compared to those of mature pears [22]. Therefore, there is a high opportunity to utilize the immature pears as a source of active components for functional food materials [22]. In order to gather high-quality mature fruits on orchard farms, immature pear fruits are discarded immediately after flowering [30]; through this process, just one cluster out of seven or eight is retained, with the rest being discarded [31]. Considering the annual production of mature pears in Korea [32], the amount of discarded immature pears is estimated to be approximately 15,000 tons per year [22], most of which are discarded [22]. To the best of our knowledge, the use of immature pear extracts to improve PM_{2.5}-induced lung disease has not been evaluated yet.

Dexamethasone (DEXA) is a representative synthetic adrenocortical steroid that exhibits approximately 20–30 times stronger anti-inflammatory effects than in vivo hydrocortisone. In addition, its effect is approximately 4–5 times better than that of prednisolone, another commonly used synthetic corticosteroid [33]. The anti-inflammatory effects of DEXA are well-known in various inflammatory respiratory diseases [16,34,35], including PM_{2.5}-induced lung damage [19]. Therefore, DEXA was selected as the positive control drug in this study.

During this study, the anti-inflammatory and lung damage improvement effects of immature Asian pear extract (IAP) were evaluated using a PM_{2.5}-induced sub-acute lung injury mouse model [1–3,16].

2. Materials and Methods

2.1. Test Material

The immature Asian pear extract (IAP; *P. pyrifolia* Nakai) used in the present study was supplied by Bioport Korea Inc., Yangsan, Republic of Korea. The immature Asian pears (2500 g) were mixed with 12,500 mL of purified water and extracted for 4 h at 100 °C. The solution was concentrated under reduced pressure using Rotavapor® R-220 (BÜCHI Labortechnik AG, Flawil, Switzerland) and spray-dried using a spray-dryer (Einsystem Co., Anyang, Republic of Korea) to obtain the powdered extract. The IAP powder, light brown in color, was dissolved in distilled water (D.W.) to prepare a stock solution at a concentration of 40 mg/mL and stored at −20 °C for further steps. The IAP powder was catalogued in the herbarium of the Medical Research Center for Herbal Convergence on Liver Disease at Daegu Haany University, Gyeongsan, Republic of Korea, with a sample number–IAP2022BPK01.

2.2. High-Performance Liquid Chromatography (HPLC)

An Agilent HPLC 1200 series (Agilent Technologies, Inc., Santa Clara, CA, USA) was employed to assess the amount of arbutin in the IAP extract using Capcell Pak C18 UG120 column (Osaka Soda Co., Ltd., Osaka, Japan) and a wavelength detector (G1314B; Agilent Technologies, Inc.). IAP extract and arbutin were dissolved in the mobile phase solvent (a mixture of acetonitrile and 10 mM KH₂PO₄ aqueous solution (1.1:98.9)) and filtered through 0.45-µm membrane filters before injection. During the analysis, the column was kept at a temperature of 30 °C, and arbutin was examined at a wavelength of 280 nm. The arbutin standard was procured from Alfa Aesar, MA, USA. For quantification, each sample was injected at a volume of 10 µL and a flow rate of 0.8 mL/min.

2.3. Animals

Seventy-two specific virus antibody-free/pathogen-free inbred male BALB/c mice, sourced from OrientBio in Seongnam, Republic of Korea, were acclimated for a period of seven days. After acclimatization, ten mice per group were allocated to six groups based on their body weight (average body weight of the normal vehicle control group: 21.23 ± 0.69 g; average body weight of the PM_{2.5} lung injury-induced experimental group: 21.19 ± 0.82 g) measured one day before the first injection of PM_{2.5} and test substance administration. The animal experiment was approved by the Animal Experiment Ethics Committee of Daegu Haany University under the approval number–DHU2022-098. Prior to test substance administration, a fasting period of 18 h was imposed on all experimental animals. On the final day leading up to the necropsy, there were no restrictions on water intake.

The experimental groups were as follows (six groups consisting of ten mice in each group):

1. Intact (vehicle) control = D.W. (10 mL/kg) administered and intranasal saline instillation (0.1 mL/kg) mice.
2. PM_{2.5} control = D.W. (10 mL/kg) administered and intranasal PM_{2.5} instillation (1 mg/kg) mice.
3. DEXA = DEXA (0.75 mg/kg) administered and intranasal PM_{2.5} instillation (1 mg/kg) mice.
4. IAP400 = IAP (400 mg/kg) administered and intranasal PM_{2.5} instillation (1 mg/kg) mice.
5. IAP200 = IAP (200 mg/kg) administered and intranasal PM_{2.5} instillation (1 mg/kg) mice.
6. IAP100 = IAP (100 mg/kg) administered and intranasal PM_{2.5} instillation (1 mg/kg) mice.

2.4. Induction of Lung Damage

To induce sub-acute lung injury, PM_{2.5} at a dose of 0.1 mL/kg (equivalent to 1 mg/kg B.W.) was twice intranasal injected into the mice, one hour before test substance administration and with a 48 h gap between (Day 0 and Day 2). To prevent excessive aggregation of PM_{2.5} molecules in the suspension, sonication was performed for 30 min using an ultrasonicator (Model 5210, Branson, St. Louis, MO, USA) before the intranasal injection.

2.5. Administration of Test Material

IAP concentrations of 40, 20, and 10 mg/mL were prepared in sterile D.W. IAP solution was orally administered to the corresponding animal once daily by utilizing a sonde attached to a 1-mL syringe for 10 days. The dose of IAP solution was set as 10 mL/kg (400, 200, and 100 mg/kg). DEXA (Sigma-Aldrich, St. Louis, MO, USA) was dissolved in sterile D.W. to prepare a 0.075 mg/mL solution and orally administered once daily for 10 days at 10 mL/kg (0.75 mg/kg) to the responding animals. To implement the similar handling, restraint, and administration stress for the normal vehicle and the PM_{2.5} control group, the same volume of vehicle and sterile D.W. was supplied orally in the same way rather than the test substance or DEXA. The DEXA dose of 0.75 mg/kg used in this experiment has been previously reported [16,19,34,35]. The highest dose of IAP selected as the test substance was 400 mg/kg, and medium and low doses were established at 200 mg/kg and 100 mg/kg, respectively, with a common ratio of two.

2.6. Removal of Lung Tissue

Lung tissue was weighed using an automatic scale (XB320M; Precisa Instrument, Dietikon, Switzerland). NB 324 3-0 sterilized nylon thread (AILEE, Busan, Republic of Korea) was used for ligating right lower secondary lobe and left secondary bronchus. The lung left lobe was used for RT-PCR (real-time reverse transcription polymerase chain reaction) analysis, macroscopic, and histopathological observations. BALF collection was performed using the right upper and middle lobes of the lungs. The long right lower lobe was utilized to analyze cytokines (IL-6, TNF- α , CXCL-1, and -2; chemokine ligand 1 and 2), the levels of matrix metalloproteinases (MMP), substance P, acetylcholine (ACh), ROS, lipid peroxidation, and antioxidant defense system.

2.7. Observation Items

B.W. and weight gain, lung weight and gross autopsy findings, aspartate transaminase (AST) and alanine transaminase (ALT) levels in serum, total cell count in BALF, total white blood cell count, leukocyte count, TNF- α , IL-6, CXCL1, CXCL2, MMP-9, MMP-12, ACh, and substance P levels in lung tissue, antioxidant defense system in lung tissue, histopathological changes in lung tissue, mucus production in lung tissue, oxidative stress and inflammation, and changes in mRNA expression associated with apoptosis were observed in this study.

2.8. Lung Gross Necropsy Findings

The percentage of congested areas in the lung was measured using the method of Lee et al. [36]. After taking a picture of the lung left lobe with a digital camera, the percentage of congestion was calculated using an automated image analyzer (iSolution FL ver 9.1; IMT i-solution Inc., Burnaby, BC, Canada).

2.9. BALF Leukocyte Fractionation

The calculation of white blood cells, neutrophils, lymphocytes, eosinophil, and monocytes was done using automatic hemocytometer following the method of Shu et al. [37]. BALF was collected from blood following the method of Glynos et al. [38].

2.10. Lung Antioxidant Defense System

Lipid peroxidation (malondialdehyde [MDA] level), ROS and GSH levels, and CAT and SOD activity were analyzed according to the methods of Glynos et al. [38], Abei [39], and Bannister [40].

2.11. Histopathological Changes in Lung Tissue

The histopathological changes, such as mean alveolar surface area (ASA; %/mm²), the number of inflammatory cells infiltrating the alveoli (cells/mm²), number of secondary bronchial mucosal periodic acid Schiff (PAS)-positive mucus-producing cells (cells/mm²),

alveolar septum thickness (μm), and secondary bronchial mucosal thickness (μm) were observed in the lung tissue following the methods of Lebargy et al. [41] and Shu et al. [37].

2.12. mRNA Expression in Lung Tissue

The mRNA expression of mucus-production-related mucin 5AC (MUC5AC) and MUC5B, oxidative stress- and inflammation-related nuclear factor (NF)- κB , p38 mitogen-activated protein kinase (MAPK), protein kinase B (Akt), phosphatase and tensin homolog (PTEN), phosphoinositide 3-kinase (PI3K), and apoptosis-related Bax and Bcl-2 genes, in lung tissue were analyzed using the methods of Deng et al. [42] and Duong et al. [43] (Table S1). Briefly, TRIzol reagent (Invitrogen, Carlsbad, CA, USA) was utilized to extract the RNA and reverse transcription of RNA was conducted using the cDNA Reverse Transcription kit (Thermo Fisher Scientific Inc., Rockford, IL, USA) following the manufacturer's instructions. RT-PCR was performed on CFX96™ Real-Time System (Bio-Rad, Hercules, CA, USA), and data were normalized using the comparative threshold cycle method [44] in comparison with the β -actin (Actb) mRNA expression, used as a control.

2.13. Statistical Analysis

All numerical data are represented as mean values \pm standard deviation, based on a sample size of ten mice in each group. Significance between groups was examined using SPSS 18.0 (SPSS Inc., Chicago, IL, USA). When there was no significance in variance observed in the Levene test, a one-way analysis of variance (ANOVA) test was employed. When the variance was significantly different, Dunnett's T3 test was performed to analyze the significance ($p < 0.05$) [45–47]. The change rate of the test substance or reference-drug-administered group compared with the PM_{2.5} control or vehicle control group, respectively, was analyzed using the following equations:

$$\text{Percentage change compared to the intact vehicle control (\%)} = \left(\frac{\text{data of PM}_{2.5} \text{ control} - \text{data of intact vehicle control mice}}{\text{data of intact vehicle control mice}} \right) \times 100 \quad (1)$$

$$\text{Percentage change compared to PM}_{2.5} \text{ control (\%)} = \left(\frac{\text{data of test material- or reference-treated mice} - \text{data of PM}_{2.5} \text{ control mice}}{\text{data of PM}_{2.5} \text{ control mice}} \right) \times 100 \quad (2)$$

3. Results

3.1. Level of Arbutin in IAP Extract

The HPLC analysis of IAP extract showed arbutin level of 8.17 mg/g (Figure 1).

3.2. Changes on the Body Weight and Gains

In the DEXA-administered group, significant weight loss ($p < 0.05$ or $p < 0.01$) was noted in comparison with the normal vehicle control group 7 days after test substance administration, and 10 days weight gain also significantly decreased ($p < 0.05$ or $p < 0.01$) in comparison with the control group. In comparison with the normal vehicle control group, no substantial differences were observed in B.W. or weight gains in any of the experimental groups. Significant ($p < 0.05$ or $p < 0.01$) changes in weight loss were observed in the DEXA-administered group 8 days after administration in comparison with the PM_{2.5} control group. The changes in weight gain over 10 days were also significantly reduced ($p < 0.05$ or $p < 0.01$) in comparison with the PM_{2.5} control group. A significant difference in B.W. and weight gains was not observed in any of the three IAP-administered groups (IAP 400, 200, and 100; Figure 2).

3.3. Findings from the Macroscopic Examination of the Lungs and Changes in Weight

The PM_{2.5} control group exhibited lung enlargement with significant local blockage and a significant increase ($p < 0.01$) in the blockage area and relative and absolute lung weight was observed in comparison with the normal vehicle control. Nevertheless, compared to the PM_{2.5} control, the three IAP groups showed a significant and dose-dependent

decrease ($p < 0.01$) in gross congestion in the lungs and both absolute and relative weights. In particular, in the IAP400 group, PM_{2.5}-induced pulmonary congestion and lung enlargement and suppression of absolute and relative lung weight increases were comparable to those in the DEXA group (Figure 3; Table 1).

Table 1. Lung weights and gross inspections in vehicle or PM_{2.5}-treated pulmonary-injured mice.

Items (Unit) Groups	Lung Weights		Congestional Regions (%)–Gross Findings
	Absolute (g)	Relative (%)	
Controls			
vehicle	0.125 ± 0.005	0.640 ± 0.033	1.64 ± 1.58
PM _{2.5}	0.185 ± 0.008 ^a	0.947 ± 0.061 ^a	68.07 ± 12.46 ^a
DEXA	0.136 ± 0.007 ^{bc}	0.735 ± 0.036 ^{ac}	8.72 ± 2.66 ^{ac}
Test substance–IAP			
400 mg/kg	0.142 ± 0.015 ^c	0.722 ± 0.080 ^c	9.02 ± 2.57 ^{ac}
200 mg/kg	0.153 ± 0.009 ^{ac}	0.771 ± 0.046 ^{ac}	31.68 ± 11.46 ^{ac}
100 mg/kg	0.161 ± 0.010 ^{ac}	0.829 ± 0.063 ^{ac}	42.49 ± 11.09 ^{ac}

Values are expressed as mean ± SD. DT3 = Dunnett's T3. ^a $p < 0.01$ and ^b $p < 0.05$ versus vehicle control via DT3 test. ^c $p < 0.01$ versus PM_{2.5} control via DT3 test.

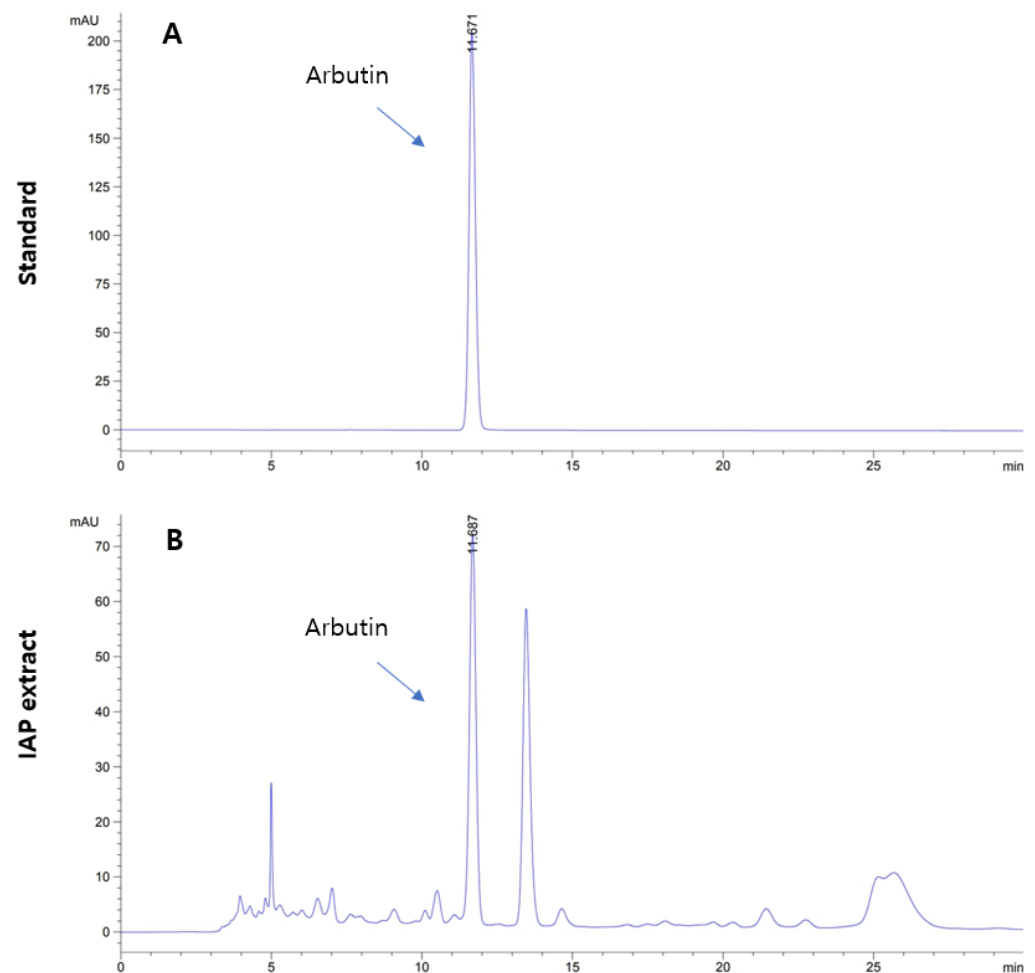


Figure 1. Profile of arbutin: (A) standard and (B) immature Asian pear extract.

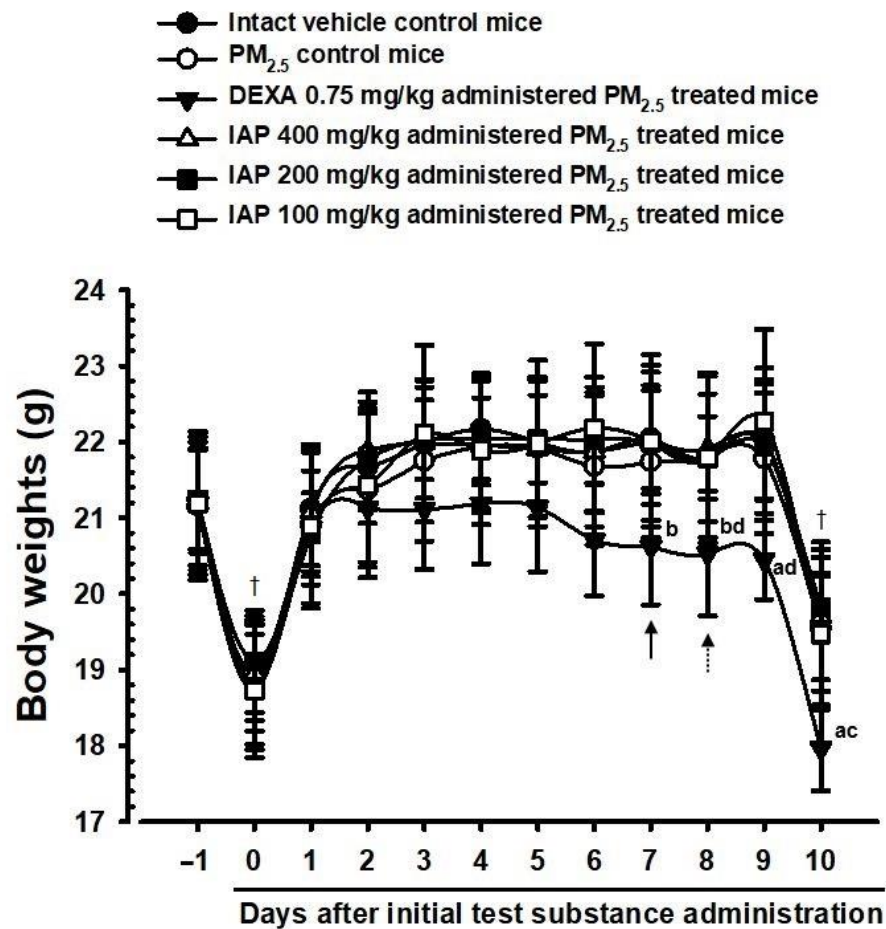


Figure 2. B.W. changes in vehicle or PM_{2.5}-treated pulmonary injured mice. THSD = Tukey’s Honest Significant Difference. Day-1 signifies one day prior to the initial administration of the test substance. Day 10 represents the day of sacrifice, which is 24 h after the last (10th) administration of the test substance. All animals underwent overnight fasting prior to both the initial administration of the test article and sacrifice (†). ^a $p < 0.01$ and ^b $p < 0.05$ versus vehicle control by THSD test. ^c $p < 0.01$ and ^d $p < 0.05$ versus PM_{2.5} control by THSD test.

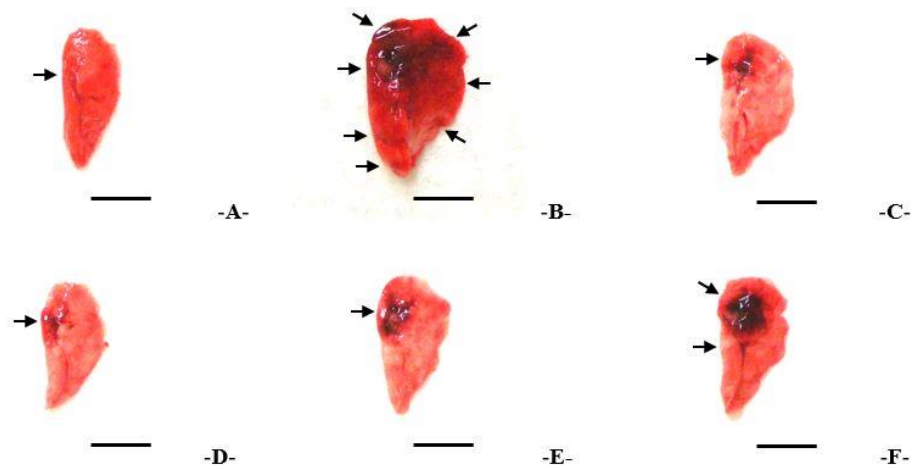


Figure 3. Representative gross left lung images, taken from vehicle or PM_{2.5}-treated pulmonary injured mice. (A) = vehicle control (D.W. PO (per oral) with saline). (B) = PM_{2.5} control (D.W. PO with PM_{2.5}). (C) = DEXA (0.75 mg/kg of DEXA PO with PM_{2.5}). (D) = IAP400 (400 mg/kg of IAP PO mice with PM_{2.5}). (E) = IAP200 (200 mg/kg of IAP PO with PM_{2.5}). (F) = IAP100 (100 mg/kg of IAP PO with PM_{2.5}). Scale bars = 6.00 mm. Arrows indicated congestion regions.

3.4. Changes in Total Cell Count, Total Leukocyte Count, and Leukocyte Differential Count in BALF

In the PM_{2.5} control, the total number of cells, neutrophils, monocytes, total leukocytes, lymphocytes, and acidophilus leukocytes in the BALF were significantly increased ($p < 0.01$) in comparison with the normal vehicle control. In contrast, the lymphocytes, total number of cells, neutrophils, total leukocytes, eosinophil, and monocytes in the BALF in all three IAP-treated groups decreased significantly ($p < 0.01$) in a dose-dependent manner. In particular, in the IAP400 group, the inhibition of an increase in the total amount of leukocytes and cells in the BALF was comparable to that in the DEXA group (Table 2).

Table 2. Cytology of BALF in vehicle or PM_{2.5}-treated pulmonary injured mice.

Items Groups	Total Cells	Total Leukocytes	Differential Counts			
			Lymphocytes	Neutrophils	Eosinophils	Monocytes
Controls						
vehicle	9.90 ± 2.02	6.70 ± 1.83	3.50 ± 1.35	1.25 ± 0.49	0.02 ± 0.02	1.28 ± 0.41
PM _{2.5}	79.70 ± 9.27 ^a	60.30 ± 6.88 ^a	35.70 ± 6.38 ^a	13.72 ± 1.51 ^a	1.85 ± 0.20 ^a	7.45 ± 0.87 ^a
DEXA	20.70 ± 3.86 ^{ac}	13.30 ± 3.33 ^{ac}	7.30 ± 3.27 ^c	2.46 ± 0.81 ^{bc}	0.28 ± 0.22 ^{bc}	2.20 ± 0.40 ^{ac}
Test substance–IAP						
400 mg/kg	21.40 ± 4.33 ^{ac}	13.80 ± 2.82 ^{ac}	7.40 ± 2.22 ^{ac}	2.64 ± 0.86 ^{ac}	0.32 ± 0.19 ^{ac}	2.32 ± 0.75 ^{bc}
200 mg/kg	43.30 ± 4.88 ^{ac}	32.20 ± 4.94 ^{ac}	19.50 ± 3.87 ^{ac}	6.77 ± 1.60 ^{ac}	0.93 ± 0.36 ^{ac}	3.70 ± 1.04 ^{ac}
100 mg/kg	54.40 ± 7.26 ^{ac}	40.00 ± 5.03 ^{ac}	23.50 ± 4.95 ^{ac}	8.74 ± 1.48 ^{ac}	1.21 ± 0.25 ^{ac}	4.79 ± 1.03 ^{ac}

Values are expressed as Mean ± SD, ×10⁴ cells/mL. BALF = Bronchoalveolar lavage fluid; DT3 = Dunnett’s T3. ^a $p < 0.01$ and ^b $p < 0.05$ versus vehicle control via DT3 test. ^c $p < 0.01$ versus PM_{2.5} control via DT3 test.

3.5. Changes in ALT and AST Levels in Serum

In contrast to the normal vehicle, all PM_{2.5}-induced lung injury experimental groups did not display significant changes in the serum AST and ALT levels. In comparison with the PM_{2.5} control group, significant changes in serum ALT and AST levels were not found in the DEXA, IAP400, IAP200, and IAP100 groups (Figure 4).

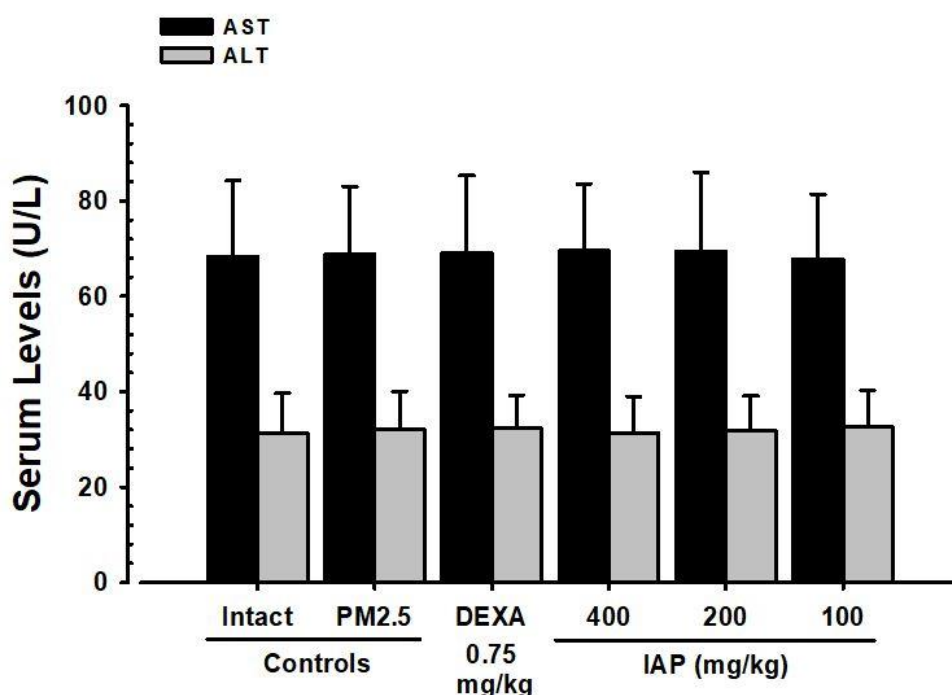


Figure 4. Serum AST and ALT levels in vehicle or PM_{2.5}-treated pulmonary-injured mice. Values are expressed mean ± SD. AST = Aspartate aminotransferase; ALT = Alanine aminotransferase.

3.6. Changes in the Levels of Cytokines IL-6, TNF- α , CXCL1, and CXCL2 in Lung Tissue

In the PM_{2.5} control group, the amount of cytokines IL-6, TNF- α , CXCL1, and CXCL2 increased significantly ($p < 0.01$) in lung tissue in comparison with the normal vehicle control group. On the other hand, compared to the PM_{2.5} control group, the levels of IL-6, TNF- α , CXCL2, and CXCL1 significantly decreased ($p < 0.01$) in groups supplied with all three doses of IAP extract. In addition, these changes were in a dose-dependent manner. In particular, in the IAP400 group, the suppression of the increase in IL-6, TNF- α , CXCL2, and CXCL1 in PM_{2.5}-induced lung tissue was comparable to that in the DEXA group (Table 3).

Table 3. Lung Cytokine-TNF- α , IL-6, CXCL1 and CXCL2 contents in vehicle or PM_{2.5}-treated pulmonary-injured mice.

Items (Unit) Groups	Lung Contents (pg/mL)			
	TNF- α	IL-6	CXCL1	CXCL2
Controls				
vehicle	30.55 \pm 10.65	30.32 \pm 12.46	32.54 \pm 10.30	17.92 \pm 5.80
PM _{2.5}	250.19 \pm 43.99 ^a	453.02 \pm 86.77 ^a	352.12 \pm 80.52 ^a	198.62 \pm 25.01 ^a
DEXA	68.92 \pm 11.80 ^{ab}	119.94 \pm 47.36 ^{ab}	97.70 \pm 21.55 ^{ab}	54.88 \pm 16.88 ^{ab}
Test substance-IAP				
400 mg/kg	69.65 \pm 12.87 ^{ab}	122.59 \pm 28.96 ^{ab}	101.86 \pm 29.95 ^{ab}	56.88 \pm 19.16 ^{ab}
200 mg/kg	115.42 \pm 28.16 ^{ab}	212.47 \pm 53.70 ^{ab}	162.32 \pm 37.62 ^{ab}	94.80 \pm 32.39 ^{ab}
100 mg/kg	156.02 \pm 26.86 ^{ab}	289.37 \pm 56.65 ^{ab}	215.30 \pm 27.37 ^{ab}	124.52 \pm 20.14 ^{ab}

Values are expressed mean \pm SD. TNF = Tumor necrosis factor; IL = interleukin; CXCL = The chemokine (C-X-C motif) ligand; DT3 = Dunnett's T3. ^a $p < 0.01$ versus vehicle control via DT3 test. ^b $p < 0.01$ versus PM_{2.5} control via DT3 test.

3.7. Changes in MMP-9 and MMP-12 Levels in Lung Tissue

In the PM_{2.5} control, the levels of MMP-9 and -12 increased significantly ($p < 0.01$) in the lung tissue when compared to the normal vehicle control group. In contrast, in a dose-dependent manner, the levels of MMP-9 and -12 decreased significantly ($p < 0.01$) in all IAP-extract-administered groups. In particular, in the IAP400 group, the suppression of the increase in MMP-9 and MMP-12 levels in PM_{2.5}-induced lung tissue was comparable to that in the DEXA group (Figure 5).

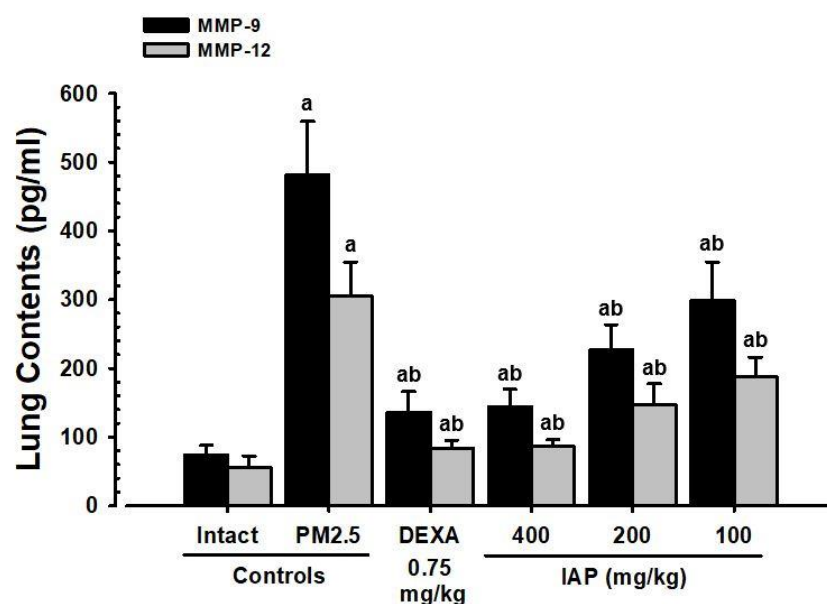


Figure 5. Lung MMP-9 and MMP-12 contents in vehicle or PM_{2.5}-treated pulmonary injured mice. Values are expressed mean \pm SD. MMP = Matrix metalloproteinase; DT3 = Dunnett's T3. ^a $p < 0.01$ versus vehicle control via DT3 test. ^b $p < 0.01$ versus PM_{2.5} control via DT3 test.

3.8. Changes in Substance P and ACh Levels in Lung Tissue

In the PM_{2.5} control, substance P and ACh levels significantly increased ($p < 0.01$) in the lung tissue compared with the normal vehicle control group. In contrast, substance P and ACh levels decrease significantly ($p < 0.01$) in the DEXA group. In all three IAP-extract-administered groups, substance P and ACh levels in the lung tissue increased significantly ($p < 0.01$) in a dose-dependent manner compared to the PM_{2.5} control (Figure 6).

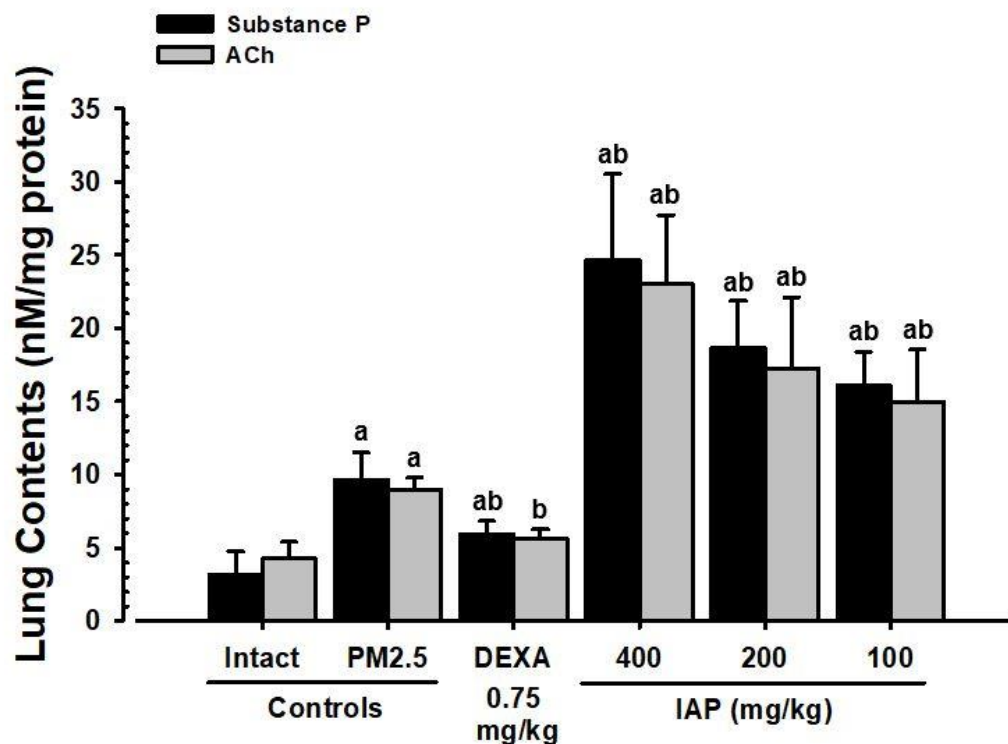


Figure 6. Lung substance P and ACh contents in vehicle or PM_{2.5}-treated pulmonary injured mice. Values are expressed mean \pm SD. ACh = Acetylcholine; DT3 = Dunnett's T3. ^a $p < 0.01$ versus vehicle control via DT3 test. ^b $p < 0.01$ versus PM_{2.5} control via DT3 test.

3.9. Changes in Lipid Peroxidation and Antioxidant Defense System in Lung Tissue

In the PM_{2.5} control group, lipid peroxidation (MDA level) and ROS increased significantly in the lung tissue ($p < 0.01$), along with a decrease in the GSH level and CAT and SOD activity when compared with the normal vehicle control group. On the other hand, a significant reduction ($p < 0.01$) in lipid peroxidation and ROS and increases in the CAT, GSH, and SOD activity were observed in the lung tissue of mice treated with all three IAP extract doses. In addition, these effects were in a dose-dependent manner. Particularly, the IAP400 group exhibited comparable antioxidant activity to the DEXA-administered group (Table 4).

3.10. Alterations in the mRNA Expression of MUC5B and MUC5AC, Which Are Related to Mucus Production in Lung Tissue

In the PM_{2.5} control group, the expression of mucus-production-related MUC5AC and MUC5B mRNA in the lung tissue significantly increased ($p < 0.01$) when compared with the normal vehicle control group. On the other hand, compared to the PM_{2.5} control group in the lung tissue, MUC5AC and MUC5B mRNA expression were reduced significantly ($p < 0.01$) in all three IAP groups in a dose-dependent manner. In particular, MUC5AC and MUC5B mRNA expression was comparable between the IAP400 and DEXA groups (Table 5).

Table 4. Lung lipid peroxidation (MDA Contents), GSH Contents, and CAT and SOD activities in vehicle or PM_{2.5}-treated pulmonary injured mice.

Items (Unit) Groups	Lung Contents (nM/mg Protein)			Lung Enzyme Activity (U/mg Protein)	
	MDA	ROS	GSH	SOD	CAT
Controls					
vehicle	3.39 ± 0.97	23.29 ± 10.28	42.70 ± 10.63	337.60 ± 51.59	75.30 ± 14.03
PM _{2.5}	21.87 ± 4.56 ^c	96.66 ± 11.71 ^a	6.36 ± 2.05 ^c	60.00 ± 18.68 ^{cd}	9.40 ± 2.01 ^c
DEXA	8.58 ± 1.44 ^{cd}	43.15 ± 8.08 ^{ab}	18.84 ± 4.56 ^{cd}	189.60 ± 39.04 ^{cd}	30.00 ± 7.32 ^{cd}
Test substance–IAP					
400 mg/kg	8.91 ± 2.46 ^{cd}	44.30 ± 9.58 ^{ab}	20.28 ± 3.86 ^{cd}	197.40 ± 34.58 ^{cd}	30.80 ± 12.45 ^{cd}
200 mg/kg	12.65 ± 2.97 ^{cd}	57.72 ± 13.11 ^{ab}	16.44 ± 3.03 ^{cd}	157.00 ± 23.97 ^{cd}	24.90 ± 7.17 ^{cd}
100 mg/kg	14.82 ± 1.69 ^{cd}	66.53 ± 13.73 ^{ab}	12.74 ± 3.28 ^{cd}	129.30 ± 14.26 ^{cd}	19.60 ± 3.10 ^{cd}

Values are expressed mean ± SD. MDA = Malondialdehyde; ROS = Reactive oxygen species; GSH = Glutathione; CAT = Catalase; SOD = Superoxide dismutase; THSD = Tukey’s Honest Significant Difference; DT3 = Dunnett’s T3. ^a *p* < 0.01 versus vehicle control by THSD test. ^b *p* < 0.01 versus PM_{2.5} control by THSD test. ^c *p* < 0.01 versus vehicle control via DT3 test. ^d *p* < 0.01 versus PM_{2.5} control via DT3 test.

Table 5. Changes in the lung tissue mRNA expressions in vehicle or PM_{2.5}-treated pulmonary injured mice.

Groups Items	Controls			Test Substance–IAP		
	Vehicle	PM _{2.5}	DEXA	400 mg/kg	200 mg/kg	100 mg/kg
MUC5AC	1.00 ± 0.07	5.15 ± 0.57 ^c	2.05 ± 0.43 ^{ce}	2.10 ± 0.43 ^{ce}	2.91 ± 0.46 ^{ce}	3.61 ± 0.76 ^{ce}
MUC5B	1.00 ± 0.06	2.95 ± 0.46 ^c	1.61 ± 0.25 ^{ce}	1.64 ± 0.22 ^{ce}	1.93 ± 0.12 ^{ce}	2.08 ± 0.19 ^{ce}
NF-κB	1.00 ± 0.06	9.20 ± 1.59 ^c	2.32 ± 0.83 ^{ce}	2.57 ± 1.16 ^{de}	4.08 ± 0.91 ^{ce}	5.62 ± 1.03 ^{ce}
p38 MAPK	1.00 ± 0.06	8.31 ± 0.88 ^c	2.33 ± 0.53 ^{ce}	2.39 ± 0.58 ^{ce}	3.89 ± 1.17 ^{ce}	5.38 ± 1.01 ^{ce}
PTEN	1.00 ± 0.07	0.28 ± 0.10 ^a	0.71 ± 0.12 ^{ab}	0.70 ± 0.08 ^{ab}	0.60 ± 0.10 ^{ab}	0.52 ± 0.05 ^{ab}
PI3K	1.00 ± 0.07	6.36 ± 0.72 ^c	1.93 ± 0.36 ^{ce}	1.99 ± 0.24 ^{ce}	3.09 ± 0.81 ^{ce}	4.33 ± 0.88 ^{ce}
Akt	1.00 ± 0.06	5.45 ± 1.43 ^c	1.83 ± 0.34 ^{ce}	1.85 ± 0.19 ^{ce}	2.65 ± 0.43 ^{ce}	3.55 ± 0.47 ^{cf}
Bcl-2	1.00 ± 0.06	0.35 ± 0.07 ^a	0.72 ± 0.11 ^{ab}	0.71 ± 0.11 ^{ab}	0.60 ± 0.10 ^{ab}	0.52 ± 0.06 ^{ab}
Bax	1.00 ± 0.06	7.18 ± 1.41 ^c	2.70 ± 0.84 ^{ce}	2.72 ± 1.23 ^{de}	3.85 ± 0.82 ^{ce}	4.75 ± 0.60 ^{ce}

Values are expressed as mean ± SD, relative expressions/β-actin mRNA. RT-PCR = Reverse transcription polymerase chain reaction; NF-κB = Nuclear factor kappa-light-chain-enhancer of activated B cells; MAPK = Mitogen-activated protein kinases; PTEN = Phosphatase and tensin homolog, PI3K = Phosphoinositide 3-kinase; Akt = Protein kinase B; Bcl-2 = B-cell lymphoma 2; Bax = Bcl-2-associated X protein; THSD = Tukey’s Honest Significant Difference; DT3 = Dunnett’s T3. ^a *p* < 0.01 versus vehicle control by DT3 test. ^b *p* < 0.01 versus PM_{2.5} control via DT3 test. ^c *p* < 0.01 and ^d *p* < 0.05 versus vehicle control by DT3 test. ^e *p* < 0.01 and ^f *p* < 0.05 versus PM_{2.5} control via DT3 test.

3.11. Alterations in the mRNA Expression of NF-κB, p38 MAPK, Akt, PI3K, and PTEN, Which Are Related to Oxidative Stress and Inflammation in Lung Tissue

In PM_{2.5} control, PI3K, NF-κB, Akt, and p38 MAPK mRNA expression increased significantly (*p* < 0.01), and PTEN mRNA expression reduced significantly (*p* < 0.01) compared to the normal vehicle control. In contrast, NF-κB, p38 MAPK, PI3K, and Akt mRNA expression reduced significantly (*p* < 0.01 or *p* < 0.05) and PTEN mRNA expression increased significantly (*p* < 0.01 or *p* < 0.05) in the lung tissue in all IAP groups in a dose-dependent manner. In particular, in the IAP400 group, p38 MAPK, inflammation-related NF-κB, Akt, PI3K, and PTEN mRNA expression and PM_{2.5}-induced oxidative stress were comparable to those in the DEXA supplied group (Table 5).

3.12. Changes in Apoptosis-Related Bcl-2 and Bax mRNA Expression in Lung Tissue

In lung tissue of the PM_{2.5} control group, apoptosis-related Bcl-2 mRNA expression significantly decreased (*p* < 0.01), while Bax mRNA expression increased in comparison with the normal vehicle control group. In contrast, Bcl-2 mRNA expression in all three IAP extract groups increased significantly (*p* < 0.01) and Bax mRNA expression decreased in a dose-dependent manner. Particularly, in the IAP400 group, the changes in PM_{2.5}-induced

apoptosis-related Bax and Bcl-2 mRNA expression in lung tissue were comparable to those in the DEXA-treated group (Table 5).

3.13. Histopathological Alterations Observed in the Lungs

In the PM_{2.5} control group, significant alveolar septal thickening was observed, attributed to inflammatory cell infiltration, accompanied by elevated secondary bronchial mucosal thickening and an increased abundance of PAS-positive mucus-producing cells. Furthermore, there was a noteworthy increase in the average alveolar septal and secondary bronchial mucosal thicknesses ($p < 0.01$), as well as an augmented number of infiltrating inflammatory cells surrounding the alveoli and an increased count of PAS-positive mucus-producing cells in the secondary bronchial mucosa. Additionally, there was an associated decrease in ASA in the PM_{2.5} control group when compared with the normal vehicle control group. Nevertheless, in all three IAP-extract-administered groups, significant increases ($p < 0.01$) in ASA and average alveolar septum thickness were observed in a dose-dependent manner. Additionally, there was a reduction in the quantity of infiltrating inflammatory cells surrounding the alveoli. Notably, in the IAP400 group, the inhibitory activity against PM_{2.5}-induced alveolar septum thickening, inflammatory cell infiltration, and ASA reduction was comparable to that observed in the DEXA-administered group. Furthermore, in line with the expectorant activity [16], all three IAP-extract-administered groups demonstrated significant increases ($p < 0.05$ or $p < 0.01$) in mean thickness of the secondary bronchial mucosa and the quantity of PAS-positive mucus-producing cells in a dose-dependent manner. Contrastingly, in the DEXA-administered group, no significant changes were observed in the average thickness of the secondary bronchial mucosa and the quantity of PAS-positive mucus-producing cells when compared to the PM_{2.5} control group (Table 6; Figure 7).

Table 6. Histomorphometric analysis of the left lobe tissue of the lungs in mice treated with the vehicle or PM_{2.5} to assess pulmonary injury.

Items Groups	Mean ASA (%/mm ²)	Mean Alveolar Septal Thickness (µm)	Mean Thickness of SB (µm)	Mean IF Cell Numbers Infiltrated in AR (×10 cells/mm ²)	PAS-Positive Cells on the SB (Cells/mm ²)
Controls					
vehicle	81.34 ± 8.03	7.52 ± 1.30	15.68 ± 1.81	62.00 ± 13.70	23.00 ± 3.16
PM _{2.5}	35.24 ± 7.72 ^a	7.25 ± 10.07 ^a	21.39 ± 1.34 ^a	732.40 ± 140.45 ^a	36.80 ± 4.54 ^a
DEXA	71.16 ± 7.40 ^b	21.77 ± 4.66 ^{ab}	21.05 ± 2.04 ^a	180.20 ± 64.34 ^{ab}	34.00 ± 12.07
Test substance–IAP					
400 mg/kg	57.25 ± 7.79 ^{ab}	21.95 ± 5.39 ^{ab}	31.60 ± 2.77 ^{ab}	184.80 ± 30.01 ^{ab}	86.20 ± 14.19 ^{ab}
200 mg/kg	60.39 ± 7.96 ^{ab}	26.37 ± 5.00 ^{ab}	28.82 ± 2.25 ^{ab}	305.00 ± 59.75 ^{ab}	69.60 ± 14.57 ^{ab}
100 mg/kg	50.54 ± 2.87 ^{ab}	30.76 ± 4.50 ^{ab}	26.59 ± 1.63 ^{ab}	399.60 ± 90.98 ^{ab}	53.60 ± 10.00 ^{ac}

Values are expressed as mean ± SD. ASA = Alveolar surface area; AR = Alveolar region; SB = Secondary bronchus mucosa; IF = Inflammatory; PAS = Periodic acid Schiff; DT3 = Dunnett’s T3. ^a $p < 0.01$ versus vehicle control via DT3 test. ^b $p < 0.01$ and ^c $p < 0.05$ versus PM_{2.5} control via DT3 test.

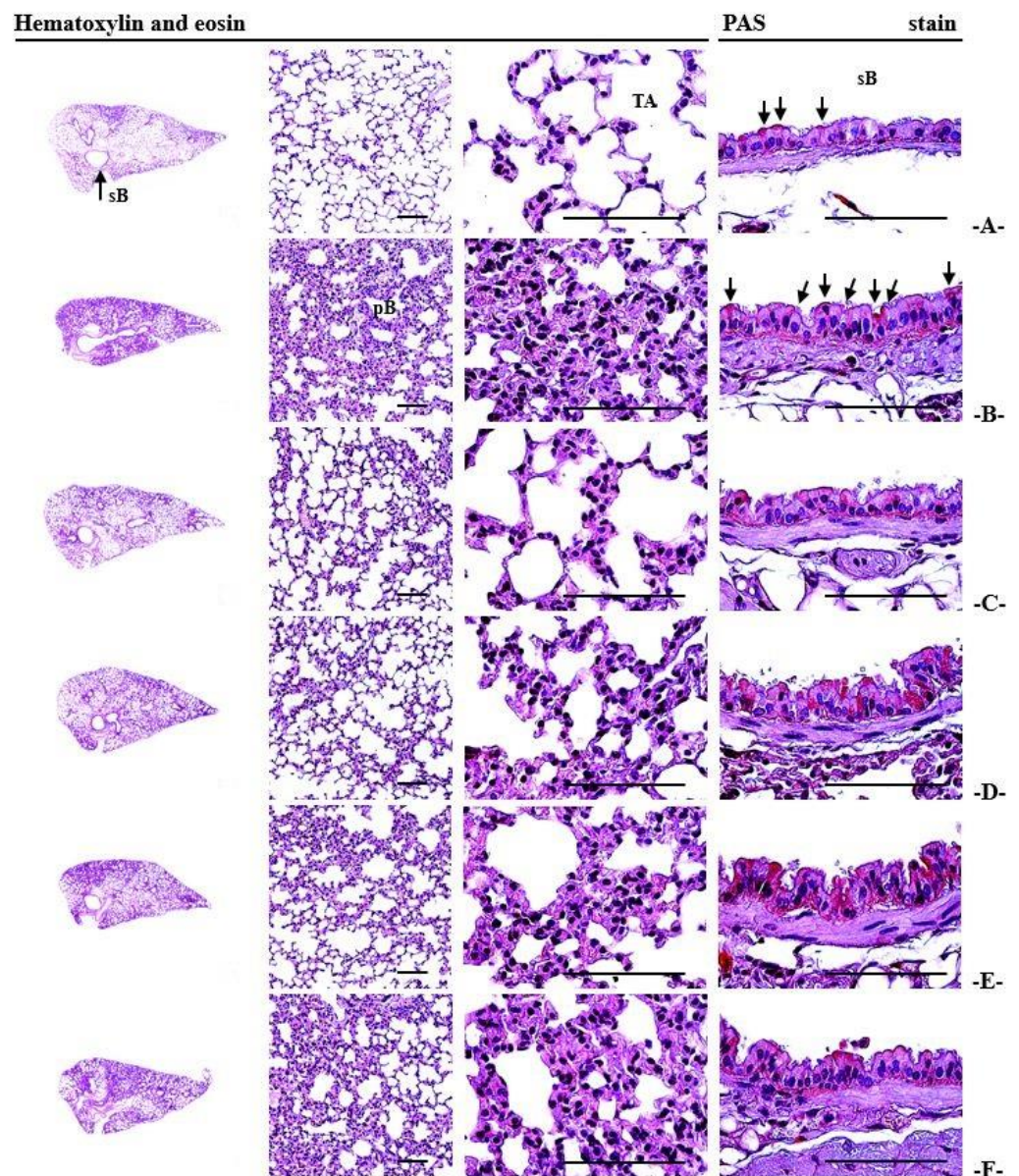


Figure 7. Representative and general histopathological profiles of the lung tissues taken from vehicle or PM_{2.5}-treated pulmonary-injured mice. ASA = Alveolar surface area; PAS = Periodic acid Schiff. sB = Secondary bronchus; pB = Primary bronchiole; TA = Terminal respiratory bronchiole-alveoli. (A) = vehicle control (DW PO (per oral) with saline). (B) = PM_{2.5} control (DW PO with PM_{2.5}). (C) = DEXA (0.75 mg/kg of DEXA PO with PM_{2.5}). (D) = IAP400 (400 mg/kg of IAP PO mice with PM_{2.5}). (E) = IAP200 (200 mg/kg of IAP PO with PM_{2.5}). (F) = IAP100 (100 mg/kg of IAP PO with PM_{2.5}). Scale bars = 200 μm; arrows indicated PAS-positive mucus-producing cells.

4. Discussion

Due to the increase in the incidence of PM-induced respiratory diseases, an alternative method for treating or preventing respiratory damage caused by PM has become necessary. In this context, the PM_{2.5}-induced lung injury model using BALB/c mouse has shown pathologies similar to human PM-induced respiratory diseases [1–3,16]. Therefore, in the present study, the dose-dependent lung damage improvement effects of IAP extract were evaluated using a PM_{2.5}-induced mouse lung injury model to find new candidates for natural drugs and functional foods that can improve lung health [1–3,16].

Significant weight loss is a well-known side effect of DEXA [16,34,48,49]. In this study, significant weight loss in the DEXA-supplied group at 7 and 8 days was noticed in

comparison with the normal vehicle and PM_{2.5} control groups, respectively. Furthermore, compared to the normal vehicle and PM_{2.5} control groups during the 10-day administration period, there was a significant decrease in B.W. and weight gain. On the other hand, in comparison with the PM_{2.5} and vehicle control groups, the weight gain and B.W. were not significantly changed in any of the three IAP-extract-administered groups, and the animal weight was similar to that of BALB/c mice of the identical age [50,51].

AST and ALT have been used as representative blood biochemical indicators to determine liver damage [52]. No significant difference in the amount of serum AST and ALT levels was noticed between the vehicle control group and the PM_{2.5}-induced lung injury experimental groups. Moreover, no significant differences in serum AST and ALT levels were noticed in DEXA, IAP400, IAP200, and IAP100 groups. All experimental mice, including the PM_{2.5} control group, showed changes in serum AST and ALT levels within the normal range for male BALB/c mice of the same age [50–52]. Hence, the current findings indicate that two intranasal injections of PM_{2.5} (1 mg/kg) 48 h apart or repeated oral administration of DEXA (0.75 mg/kg) or IAP (400, 200, or 100 mg/kg) one time each day during 10 days does not cause serious liver toxicity in mice.

Lung weight is commonly used as an indicator for observing pulmonary edema as a result of vascular leakage [16,34,53]. Similar to the ovalbumin-induced asthma model [54,55] in PM_{2.5}-induced mice, as part of the inflammatory response, the vascular endothelial cells' binding force can weaken, resulting in pulmonary edema as an effect of vascular leakage increase [2,3,16]. Following intranasal injection of PM_{2.5}, lung enlargement with pronounced local congestion, indicating pulmonary edema, was noted, and significant increases in gross congestion and absolute and relative lung weights were observed compared to the normal vehicle control group. Nevertheless, in all IAP-extract-administered groups, significant reductions in pulmonary congestion (visibly observed) and lung weights (relative and absolute) were observed in a dose-dependent manner. Particularly, PM_{2.5}-induced lung blockage, weight gain (relative and absolute), and lung enlargement were comparable between the IAP400 and DEXA groups. These results provide evidence that the oral administration of IAP extract significantly and dose-dependently suppresses PM_{2.5}-induced pulmonary edema.

Regarding inflammatory lung damage caused by intranasal injection of PM_{2.5}, there were significant increases in lymphocytes, neutrophils, amount of total leukocytes, eosinophil, monocytes, and total cell number in BALF. In contrast, in all three IAP-extract-administered groups, the number of cells, white blood cells, lymphocytes, monocytes, neutrophils, and eosinophils in BALF significantly decreased in a dose-dependent manner. In particular, the amount of leukocytes and cells in BALF of the IAP400 group were comparable to those of the DEXA group, indicating that the oral administration of IAP extract significantly suppresses lung damage in PM_{2.5}-induced inflammation.

Mucus, present on the surface of the respiratory system, serves as the primary defense against various foreign substances and infectious agents. Mucin, a glycoprotein, is a crucial component of mucus [56,57]. The cleansing action of the microcilia in the respiratory system is directly influenced by the quantity and viscosity of mucin. In other words, impaired cleansing action of the microcilia is indicated by the presence of a large amount of mucin with high viscosity [58]. MUC5AC and MUC5B are the predominant polymeric substances secreted by the respiratory system [56,57], and alterations in the expression of MUC5AC and MUC5B are induced in various respiratory diseases [59–61]. Particularly, PM_{2.5} is known to promote mucin production by increasing the expression of MUC5AC and MUC5B mRNA, resulting in the formation of high-viscosity sputum [16,56,57].

In the respiratory system, secretion is primarily regulated through the nervous system [62]. Stimulation or excitation of the vagus nerve leads to the local secretion of ACh and significant glandular secretion [63]. Indeed, Substance P is a well-known representative factor that promotes serous secretion in the respiratory system [64–66]. Hence, serous secretion in the respiratory system is primarily regulated by ACh and Substance P [62,63]. Furthermore, Substance P also functions as a neurogenic inflammatory factor in the respi-

ratory system [67]. The inhalation of PM_{2.5} leads to a noteworthy increase in Substance P levels [68,69]. Moreover, PM_{2.5} exposure escalates vascular permeability, contributing to the inflammatory response [2,3], as a result causing an increase in ACh levels, which acts as a vasorelaxant factor [16,70]. However, in PM_{2.5}-induced lung injury mice, the vascular reactivity to ACh notably diminishes [71]. In the current experiment, the PM_{2.5} control group exhibited heightened production of high-viscosity mucus, driven by increased levels of ACh and substance P [16]. Additionally, there was an increase in mRNA expression of MUC5AC and MUC5B [16,64,65], contributing to a pronounced neurogenic inflammatory response within lung tissue. On the contrary, as part of the mucolytic expectorant activity, significant increases in the secretion-promoting factors Substance P and ACh [16,62,63] were observed. Additionally, a reduction in mRNA expression of mucus-production-related genes MUC5AC and MUC5B [16,56,57] in lung tissue was observed in a dose-dependent manner in all three IAP-extract-administered groups. These results verify that the oral administration of IAP extract (400, 200, or 100 mg/kg) results in mucolytic expectorant activity through mucin-reducing effects by decreasing MUC5AC and MUC5B mRNA expression, as well as promoting serous secretion by increasing substance P and ACh production. In contrast, a significant reduction in MUC5AC and MUC5B mRNA expression was observed in the DEXA group. These expression levels were comparable to those observed in the IAP400 group. However, the levels of substance P and ACh were significantly decreased in the DEXA group when compared to the PM_{2.5} control group.

The inhalation of PM_{2.5} triggers an oxidative stress-induced inflammatory response characterized by increased lipid peroxidation and a depletion of the antioxidant defense system, leading to decreased GSH, CAT, and SOD activity [1–3,13,16,72,73]. As a consequence of the inflammatory response, there is an upsurge in the secretion of cytokines, such as TNF- α , IL-6, CXCL1, and CXCL2 [1–3,13,16,72,73]. Indeed, lipid peroxidation is an autocatalytic process that results in the oxidative degradation of cell membranes [74,75]. Destruction of the cell membrane by lipid peroxidation promotes the formation of toxic reactive aldehyde metabolites and cell death represented by MDA, i.e., free radicals [76,77]. Oxidative damage can affect a range of biological macromolecules, including but not limited to proteins, DNA, and lipids, as a result of exposure to various forms of ROS [77,78]. During the lipid peroxidation process, the amount of MDA produced is used to determine the lipid peroxidation index [77]. As an endogenous antioxidant, it serves as a representative molecule that effectively eliminates ROS even at low concentrations within cells, thereby controlling tissue damage [79]. SOD is also an endogenous antioxidant enzyme that acts as part of a cell's enzymatic defense system, and CAT is a representative endogenous antioxidant enzyme that converts toxic hydrogen peroxide (H₂O₂) to harmless water (H₂O) [80]. The decrease in GSH, SOD and CAT activity indicates the failure of compensatory action due to oxidative stress induced by inhalation of PM_{2.5} [1–3,13,16].

PM_{2.5} causes an increase in the level of chemotactic cytokines CXCL1 and CXCL2 in blood and respiratory tissues as part of an inflammatory response [16,72,73]. NF- κ B is recognized as having an important role in inflammation associated with some adhesion molecules, ROS, and binds to promoters encoded in IL-6, IL-1, and TNF- α to trigger their transcription [81,82]. It also regulates various cytokine expressions, including IL-6, IL-10, CXCL1, and CXCL2, which are directly related to the inflammatory responses [83]. The amount of TNF- α , IL-6, CXCL1, and CXCL2 increases with an increase in NF- κ B expression even during PM_{2.5}-induced lung injury [16,72]. Furthermore, p38 MAPK, PI3K, and Akt signaling pathways are involved in ROS-induced oxidative stress caused by PM_{2.5}-induced lung injury [42,84]. In particular, Akt activity triggers an inflammatory response by increasing the secretion of inflammatory chemotactic factor CXCL1 through an increase in NF- κ B expression [85]. PTEN is a representative tumor suppressor gene, and abnormalities in PTEN cause the pathogenesis of several malignant tumors [86–88]. The MAPK signaling pathway regulates the expression of PTEN [89]. In other words, the inhibition of the MAPK signaling pathway maintains PTEN expression and significantly reduces the occurrence of malignant tumors [88,90]. The possibility of malignant tumor formation

increases in PM_{2.5}-treated lung tissues, as there is a significant decrease in the expression of the tumor suppressor gene PTEN [91,92]. In the current study, the intranasal injection of PM_{2.5} (1 mg/kg) showed significant lipid peroxidation in lung tissue, increased MDA and ROS levels, decreased GSH, CAT, and SOD activity, increased inflammatory cytokines TNF- α , IL-6, CXCL-1, and -2, together with inflammation-related NF- κ B and oxidative stress, increased PI3K, Akt, and p38 MAPK expression, and decreased PTEN expression. Meanwhile, oxidative stress and inflammatory lung damage through PM_{2.5}-induced NF- κ B, p38 MAPK, and PI3K/Akt expression decreased in a dose-dependent manner in all three IAP-extract-administered groups. The IAP400 group showed anti-inflammatory and antioxidant activity comparable to that in the DEXA group, suppressing PM_{2.5}-induced sub-acute lung injury. The results of this study indicate that the IAP extract administration dose-dependently inhibits the PM_{2.5}-induced oxidative stress and inflammatory lung damage via antioxidant and anti-inflammatory activities by the reduction of p38 MAPK, NF- κ B, and PI3K/Akt expression.

MMPs are a group of structurally similar endopeptidases [93]. MMPs play an important role in tumor invasion, tissue morphogenesis, skin aging, angiogenesis, arthritis, and tissue repair, as they cause the degradation of various extracellular matrices [94,95]. MMPs can be subdivided into collagen-degrading enzymes, gelatinases, matrix-lysing enzymes, membranous MMPs, and various other types according to their structural characteristics and substrates [96,97]. PM_{2.5} increases the expression of various MMPs, especially MMP-9 and MMP-12, as part of an inflammatory response, destroying the parenchyma of the surrounding respiratory system and causing respiratory distress through airway damage [16,93,98,99]. In this experiment, there were significant increases in MMP-9 and -12 levels in the lung tissue of the PM_{2.5} control group compared to the normal vehicle control group. However, in contrast, the levels of MMP-9 and -12 in the lung tissue of all IAP-extract-administered groups were significantly reduced in a dose-dependent manner. Notably, the IAP400 group exhibited similar levels of MMP-9 and MMP-12 in PM_{2.5}-induced lung tissue compared to the DEXA group. These findings indicate that oral administration of IAP extract can effectively mitigate PM_{2.5}-induced airway damage in a dose-dependent manner by reducing MMP-9 and MMP-12 expression.

Indeed, excessive ROS imposes oxidative stress on proteins and lipids within the mitochondrial membrane, leading to severe damage. This damage may include loss of membrane potential, increased membrane permeability, and release of cytochrome c [100], activating caspase-3 and mitochondria-dependent apoptosis [101]. Oxidative stress caused by PM_{2.5} induces mitochondria-dependent apoptosis [102]. Exactly, in the context of mitochondria-dependent apoptosis, Bax and Bcl-2 serve as representative pro-apoptotic and anti-apoptotic proteins, respectively. Bax plays a critical role in this process by inducing the loss of mitochondrial membrane potential, leading to the activation of caspase-3 and the release of cytochrome c, ultimately triggering apoptosis [103]. Exposure to PM_{2.5} affects a rise in Bax expression and a decrease in Bcl-2 expression [16,100,101]. In this experiment, the expression of apoptosis-related Bcl-2 mRNA was significantly decreased, and the expression of Bax mRNA was significantly increased in the lung tissue of the PM_{2.5} control group compared to the normal vehicle control group. On the other hand, the expression of Bcl-2 mRNA was increased, and the expression of Bax mRNA was decreased in the lung tissue of all three IAP-extract-administered mice, in a dose-dependent manner. In particular, Bcl-2 and Bax mRNA expression in PM_{2.5}-induced lung tissue was comparable between the IAP400 and DEXA groups. These results show that the oral administration of IAP extract can dose-dependently suppress lung damage caused by PM_{2.5}-induced apoptosis by regulating Bax and Bcl-2 mRNA expression.

The air space area (ASA; %/mm²) could act as an indirect indicator to measure the gas exchange capacity histomorphometrically. A reduction in gas exchange surface area decreases ASA, indicating a decrease in lung function. In several lung diseases, a decrease in ASA has been noticed histopathologically [16,34,49,104]. PAS staining is a classic histochemical technique utilized to selectively stain mucus-secreting cells. An increase in PAS

staining indicates heightened activity of mucus-producing cells [16,105,106]. Along with bronchial mucosal thickening, an increase in the number of PAS-positive mucus-producing cells in the bronchial mucosa is histopathologically considered as an indicator of an expectorant effect [16,106,107]. Consistent with the findings of previous drug efficacy experiments using a PM_{2.5}-induced lung injury model [2,3,13,16], the present study also demonstrated that intranasal injection of PM_{2.5} (1 mg/kg) results in histopathologically significant lesions, including alveolar septum thickening due to inflammatory cell infiltration, and secondary bronchial mucosal thickening. Additionally, there was an increase in PAS-positive mucus-producing cells. Compared to the vehicle control group, the PM_{2.5}-induced lung injury mouse model exhibited significant increases in average alveolar septum and secondary bronchial mucosal thickness, as well as in the number of infiltrating inflammatory cells around the alveoli and amount of PAS-positive mucus-producing cells in the secondary bronchial mucosa. Concurrently, there were associated reductions in ASA in lung tissues. In contrast to the PM_{2.5} control group, all IAP-extract-administered groups demonstrated notable increases in ASA and average alveolar septum thickness, along with a decrease in the number of infiltrating inflammatory cells surrounding the alveoli. The observed changes were in a dose-dependent manner. In particular, in the IAP400 group, the inhibition of PM_{2.5}-induced alveolar septum thickening and inflammatory cell infiltration and related ASA reduction were comparable to those in the DEXA group. Also, in a part of expectorant activity [16,106,107], significant increases in the amount of PAS-positive mucus-producing cells and the mean thickness of secondary bronchial mucosa were found in a dose-dependent manner in all IAP-extract-administered groups. However, in the DEXA group, compared to the PM_{2.5} control group, significant changes in the amount of PAS-positive mucus-producing cells and average thickness of secondary bronchial mucosa were not observed. These findings show that the administration of IAP extract significantly activates not only the anti-inflammatory activity but also the mucolytic expectorant effect through the stimulation of gland fluid production in PM_{2.5}-induced sub-acute lung injury in a dose-dependent manner.

In addition, IAP extract showed expectorant effects on PM_{2.5}-induced sub-acute pulmonary injury in mice [108] and an alleviation effect on ovalbumin-induced asthma [109]. Based on the findings of this study, IAP extract shows promise as a potential natural drug or health-functional food for enhancing respiratory function and mitigating the impact of respiratory disorders caused by PM_{2.5}-induced lung injury. In this study, during HPLC analysis of IAP extract, substances corresponding to the remaining peaks, excluding arbutin, were not chemically identified. While the protective effect of IAP extract against lung injury was confirmed in this study, the protective effect of each HPLC peak could be studied in the future.

5. Conclusions

Stress-induced inflammatory lung damage through the increased expression of PM_{2.5}-induced PI3K/Akt and p38 MAPK mRNA was significantly suppressed via the administration of IAP extract (400–100 mg/kg) in a dose-dependent manner. As part of the mucolytic expectorant activity of IAP extract, significant increases in the amount of PAS-positive mucus-producing cells and mean thickness of the secondary bronchial mucosa were observed as compared to the PM_{2.5} control group. Furthermore, IAP extract administration promoted serous fluid production in lung tissue, increased substance P and ACh levels, and decreased mucus production-related expression of MUC5AC and MUC5B mRNA in a dose-dependent manner. In particular, the administration of 400 mg/kg of IAP extract showed anti-inflammatory and antioxidative activity similar to that observed in the DEXA (0.75 mg/kg) administered group and significantly suppressed the PM_{2.5}-induced sub-acute lung injury. Unlike DEXA, IAP extract exhibited mucolytic expectorant activity by promoting meaningful serous fluid production (increase in substance P and ACh production and decrease in MUC5AC and MUC5B mRNA expression); therefore, it has

great potential as a new pharmaceutical or health-functional food materials for improving effective respiratory function.

Supplementary Materials: The following supporting information can be downloaded at <https://www.mdpi.com/article/10.3390/app13179578/s1>, Table S1: Oligonucleotides for quantitative RT-PCR analysis.

Author Contributions: Conceptualization, K.-Y.K., S.-K.K. and J.-S.C.; methodology, S.S., E.-J.H. and S.-K.K.; software, J.-H.L. and M.-U.K.; validation, K.-Y.K. and S.S.; formal analysis, J.-H.L., M.-U.K. and S.-K.K.; investigation, M.-U.K. and J.-H.L.; resources, K.-Y.K.; data curation, M.-U.K. and S.-K.K.; writing, original draft preparation, M.-R.K., J.-H.L. and S.-K.K.; writing, review and editing, S.-K.K. and J.-S.C.; visualization, M.-R.K., J.-H.L. and M.-U.K.; supervision, S.-K.K. and J.-S.C.; project administration, K.-Y.K. and J.-S.C.; funding acquisition, K.-Y.K. and J.-S.C. All authors have read and agreed to the published version of the manuscript.

Funding: This study was supported by the Korea Institute of Planning and Evaluation for Technology in Food, Agriculture, Forestry (IPET) through the High Value-added Food Technology Development Program, funded by the Ministry of Agriculture, Food and Rural Affairs (MAFRA) (grant no. 122027-2).

Institutional Review Board Statement: The animal experiment was approved by the Animal Experiment Ethics Committee of Daegu Haany University with approval number DHU2022-098 (21 October 2022).

Informed Consent Statement: Not applicable.

Data Availability Statement: The data used to support the findings of this study are available from the corresponding author upon request.

Conflicts of Interest: The authors declare no conflict of interest.

References

1. Fernando, I.P.S.; Jayawardena, T.U.; Kim, H.S.; Lee, W.W.; Vaas, A.P.J.P.; De Silva, H.I.C.; Abayaweera, G.S.; Nanayakkara, C.M.; Abeytunga, D.T.U.; Lee, D.S.; et al. Beijing urban particulate matter-induced injury and inflammation in human lung epithelial cells and the protective effects of fucosterol from *Sargassum binderi* (Sonder ex J. Agardh). *Environ. Res.* **2019**, *172*, 150–158. [[CrossRef](#)]
2. Lee, W.; Ku, S.K.; Kim, J.E.; Cho, S.H.; Song, G.Y.; Bae, J.S. Inhibitory effects of protopanaxatriol type ginsenoside fraction (Rgx365) on particulate matter-induced pulmonary injury. *J. Toxicol. Environ. Health A* **2019**, *82*, 338–350. [[CrossRef](#)] [[PubMed](#)]
3. Lee, W.; Ku, S.K.; Kim, J.E.; Cho, S.H.; Song, G.Y.; Bae, J.S. Inhibitory effects of black ginseng on particulate matter-induced pulmonary injury. *Am. J. Chin. Med.* **2019**, *47*, 1237–1251. [[CrossRef](#)] [[PubMed](#)]
4. Zhuang, G.; Guo, J.; Yuan, H.; Zhao, C. The compositions, sources, and size distribution of the dust storm from China in spring of 2000 and its impact on the global environment. *Chin. Sci. Bull.* **2001**, *46*, 895–900. [[CrossRef](#)]
5. Wang, W.; Primbs, T.; Tao, S.; Simonich, S.L. Atmospheric particulate matter pollution during the 2008 Beijing Olympics. *Environ. Sci. Technol.* **2009**, *43*, 5314–5320. [[CrossRef](#)] [[PubMed](#)]
6. Huang, X.F.; He, L.Y.; Hu, M.; Zhang, Y.H. Annual variation of particulate organic compounds in PM_{2.5} in the urban atmosphere of Beijing. *Atmos. Environ.* **2006**, *40*, 2449–2458. [[CrossRef](#)]
7. Lv, B.; Zhang, B.; Bai, Y. A systematic analysis of PM_{2.5} in Beijing and its sources from 2000 to 2012. *Atmos. Environ.* **2016**, *124*, 98–108. [[CrossRef](#)]
8. Chiu, H.F.; Tsai, S.S.; Yang, C.Y. Short-term effects of fine particulate air pollution on hospital admissions for hypertension: A time-stratified case-crossover study in Taipei. *J. Toxicol. Environ. Health A* **2017**, *80*, 258–265. [[CrossRef](#)]
9. WHO. Air Pollution. Available online: https://www.who.int/health-topics/air-pollution#tab=tab_1 (accessed on 15 December 2022).
10. Nunes, C.; Pereira, A.M.; Morais-Almeida, M. Asthma costs and social impact. *Asthma Res. Pract.* **2017**, *3*, 1. [[CrossRef](#)]
11. Wang, G.; Huang, L.; Gao, S.; Gao, S.; Wang, L. Measurements of PM₁₀ and PM_{2.5} in urban area of Nanjing, China and the assessment of pulmonary deposition of particle mass. *Chemosphere* **2002**, *48*, 689–695. [[CrossRef](#)]
12. Schaumann, F.; Borm, P.J.; Herbrich, A.; Knoch, J.; Pitz, M.; Schins, R.P.; Luettig, B.; Hohlfeld, J.M.; Heinrich, J.; Krug, N. Metal-rich ambient particles (particulate matter 2.5) cause airway inflammation in healthy subjects. *Am. J. Respir. Crit. Care Med.* **2004**, *170*, 898–903. [[CrossRef](#)] [[PubMed](#)]
13. Wang, F.; Wang, R.; Liu, H. The acute pulmonary toxicity in mice induced by *Staphylococcus aureus*, particulate matter, and their combination. *Exp. Anim.* **2019**, *68*, 159–168. [[CrossRef](#)] [[PubMed](#)]
14. Pozzi, R.; De Berardis, B.; Paoletti, L.; Guastadisegni, C. Inflammatory mediators induced by coarse (PM_{2.5-10}) and fine (PM_{2.5}) urban air particles in RAW 264.7 cells. *Toxicology* **2003**, *183*, 243–254. [[CrossRef](#)]

15. Valavanidis, A.; Vlachogianni, T.; Fiotakis, K.; Loidas, S. Pulmonary oxidative stress, inflammation and cancer: Respirable particulate matter, fibrous dusts and ozone as major causes of lung carcinogenesis through reactive oxygen species mechanisms. *Int. J. Environ. Res. Public Health* **2013**, *10*, 3886–3907. [[CrossRef](#)] [[PubMed](#)]
16. Park, S.M.; Jung, C.J.; Lee, D.G.; Choi, B.R.; Ku, T.H.; La, I.J.; Cho, I.J.; Ku, S.K. *Adenophora stricta* root extract protects lung injury from exposure to particulate matter 2.5 in mice. *Antioxidants* **2022**, *11*, 1376. [[CrossRef](#)] [[PubMed](#)]
17. Devipriya, D.; Gowri, S.; Nideesh, T.R. Hepatoprotective effect of *Pterocarpus marsupium* against carbon tetrachloride induced damage in albino rats. *Anc. Sci. Life* **2007**, *27*, 19–25. [[PubMed](#)]
18. Kim, H.S.; Park, S.I.; Choi, S.H.; Song, C.H.; Park, S.J.; Shin, Y.K.; Han, C.H.; Lee, Y.J.; Ku, S.K. Single oral dose toxicity test of blue honeysuckle concentrate in mice. *Toxicol. Res.* **2015**, *31*, 61–68. [[CrossRef](#)]
19. Wang, P.; Liu, H.; Fan, X.; Zhu, Z.; Zhu, Y. Effect of San'ao decoction on aggravated asthma mice model induced by PM_{2.5} and TRPA1/TRPV1 expressions. *J. Ethnopharmacol.* **2019**, *236*, 82–90. [[CrossRef](#)]
20. Lin, L.Z.; Harnly, J.M. Phenolic compounds and chromatographic profiles of pear skins (*Pyrus* spp.). *J. Agric. Food Chem.* **2008**, *56*, 9094–9101. [[CrossRef](#)]
21. Tanrioven, D.; Eksi, A. Phenolic compounds in pear juice from different cultivars. *Food Chem.* **2005**, *93*, 89–93. [[CrossRef](#)]
22. Lee, S.W.; Cho, J.Y.; Jeong, H.Y.; Na, T.W.; Lee, S.H.; Moon, J.H. Enhancement of antioxidative and antimicrobial activities of immature pear (*Pyrus pyrifolia* cv. Niitaka) fruits by fermentation with *Leuconostoc mesenteroides*. *Food Sci. Biotechnol.* **2016**, *25*, 1719–1726. [[CrossRef](#)] [[PubMed](#)]
23. Lee, K.H.; Cho, J.Y.; Lee, H.J.; Ma, Y.K.; Kwon, J.; Park, S.H.; Lee, S.H.; Cho, J.A.; Kim, W.S.; Park, K.H.; et al. Hydroxycinnamoylmalic acids and their methyl esters from pear (*Pyrus pyrifolia* Nakai) fruit peel. *J. Agric. Food Chem.* **2011**, *59*, 10124–10128. [[CrossRef](#)] [[PubMed](#)]
24. Cho, J.Y.; Kim, C.H.; Lee, H.J.; Lee, S.H.; Cho, J.A.; Kim, W.S.; Park, K.H.; Moon, J.H. Caffeoyl triterpenes from pear (*Pyrus pyrifolia* Nakai) fruit peels and their antioxidative activities against oxidation of rat blood plasma. *J. Agric. Food Chem.* **2013**, *61*, 4563–4569. [[CrossRef](#)] [[PubMed](#)]
25. Lee, K.H.; Cho, J.Y.; Lee, H.J.; Park, K.Y.; Ma, Y.K.; Lee, S.H.; Cho, J.A.; Kim, W.S.; Park, K.H.; Moon, J.H. Isolation and identification of phenolic compounds from an Asian pear (*Pyrus pyrifolia* Nakai) fruit peel. *Food Sci. Biotechnol.* **2011**, *20*, 1539–1545. [[CrossRef](#)]
26. Lee, H.S.; Isse, T.; Kawamoto, T.; Baik, H.W.; Park, J.Y.; Yang, M. Effect of Korean pear (*Pyrus pyrifolia* cv. Shingo) juice on hangover severity following alcohol consumption. *Food Chem. Toxicol.* **2013**, *58*, 101–106. [[CrossRef](#)] [[PubMed](#)]
27. Lee, Y.G.; Cho, J.Y.; Kim, C.M.; Jeong, H.Y.; Lee, D.I.; Kim, S.R.; Lee, S.H.; Kim, W.S.; Park, K.H.; Moon, J.H. Isolation and identification of 3 low-molecular compounds from pear (*Pyrus pyrifolia* Nakai cv. Chuhwangbae) fruit peel. *Korean J. Food Sci. Technol.* **2013**, *45*, 174–179. [[CrossRef](#)]
28. Cho, J.Y.; Lee, Y.G.; Lee, S.H.; Kim, W.S.; Park, K.H.; Moon, J.H. An ether and three ester derivatives of phenylpropanoid from pear (*Pyrus pyrifolia* Nakai cv. Chuhwangbae) fruit and their radical-scavenging activity. *Food Sci. Biotechnol.* **2014**, *23*, 253–259. [[CrossRef](#)]
29. Cho, J.Y.; Kim, E.H.; Yun, H.R.; Jeong, H.Y.; Lee, Y.G.; Kim, W.S.; Moon, J.H. Change in chemical constituents and free radical-scavenging activity during pear (*Pyrus pyrifolia*) cultivar fruit development. *Biosci. Biotechnol. Biochem.* **2015**, *79*, 260–270. [[CrossRef](#)]
30. Lee, Y.G.; Cho, J.Y.; Park, J.; Lee, S.H.; Kim, W.S.; Park, K.H.; Moon, J.H. Large-scale isolation of highly pure malaxinic acid from immature pear (*Pyrus pyrifolia* Nakai) fruit. *Food Sci. Biotechnol.* **2013**, *22*, 1539–1545. [[CrossRef](#)]
31. Lee, S.W.; Lee, Y.G.; Cho, J.Y.; Kim, Y.C.; Lee, S.H.; Kim, W.S.; Moon, J.H. Establishment of a simple method for purification of high purity chlorogenic acid from immature fruit of pear (*Pyrus pyrifolia* Nakai). *Appl. Biol. Chem.* **2015**, *58*, 335–341. [[CrossRef](#)]
32. Cho, J.Y.; Park, K.Y.; Lee, K.H.; Lee, H.J.; Lee, S.H.; Cho, J.A.; Kim, W.S.; Shin, S.C.; Park, K.H.; Moon, J.H. Recovery of arbutin in high purity from fruit peels of pear (*Pyrus pyrifolia* Nakai). *Food Sci. Biotechnol.* **2011**, *20*, 801–807. [[CrossRef](#)]
33. Hollander, J.L. Clinical use of dexamethasone: Role in treatment of patients with arthritis. *J. Am. Med. Assoc.* **1960**, *172*, 306–310. [[CrossRef](#)] [[PubMed](#)]
34. Min, B.G.; Park, S.M.; Choi, Y.W.; Ku, S.K.; Cho, I.J.; Kim, Y.W.; Byun, S.H.; Park, C.A.; Park, S.J.; Na, M.; et al. Effects of *Pelargonium sidoides* and *Coptis Rhizoma* 2:1 mixed formula (PS+CR) on ovalbumin-induced asthma in mice. *Evid. Based Complement. Altern. Med.* **2020**, *2020*, 9135637. [[CrossRef](#)] [[PubMed](#)]
35. Piao, C.H.; Fan, Y.J.; Nguyen, T.V.; Song, C.H.; Chai, O.H. Mangiferin alleviates ovalbumin-induced allergic rhinitis via Nrf2/HO-1/NF-κB signaling pathways. *Int. J. Mol. Sci.* **2020**, *21*, 3415. [[CrossRef](#)] [[PubMed](#)]
36. Lee, Y.S.; Cho, I.J.; Kim, J.W.; Lee, M.K.; Ku, S.K.; Choi, J.S.; Lee, H.J. Hepatoprotective effects of blue honeysuckle on CCl₄-induced acute liver damaged mice. *Food Sci. Nutr.* **2019**, *7*, 322–338. [[CrossRef](#)] [[PubMed](#)]
37. Shu, J.; Li, D.; Ouyang, H.; Huang, J.; Long, Z.; Liang, Z.; Chen, Y.; Chen, Y.; Zheng, Q.; Kuang, M.; et al. Comparison and evaluation of two different methods to establish the cigarette smoke exposure mouse model of COPD. *Sci. Rep.* **2017**, *7*, 15454. [[CrossRef](#)] [[PubMed](#)]
38. Glynos, C.; Bibli, S.I.; Katsaounou, P.; Pavlidou, A.; Magkou, C.; Karavana, V.; Topouzis, S.; Kalomenidis, I.; Zakyntinos, S.; Papapetropoulos, A. Comparison of the effects of e-cigarette vapor with cigarette smoke on lung function and inflammation in mice. *Am. J. Physiol. Lung Cell Mol. Physiol.* **2018**, *315*, L662–L672. [[CrossRef](#)] [[PubMed](#)]
39. Aebi, H. Catalase. In *Methods in Enzymatic Analysis*; Bergmeyer, H.U., Ed.; Academic Press: New York, NY, USA, 1974; pp. 673–686.
40. Bannister, J.V.; Calabrese, L. Assays for superoxide dismutase. In *Methods of Biochemical Analysis*; Glick, D., Ed.; John Wiley & Sons, Inc.: Hoboken, NJ, USA, 1987; Volume 32, pp. 279–312.

41. Lebargy, F.; Lenormand, E.; Pariente, R.; Fournier, M. Morphological changes in rat tracheal mucosa immediately after antigen challenge. *Bull. Eur. Physiopathol. Respir.* **1987**, *23*, 417–421.
42. Deng, X.; Rui, W.; Zhang, F.; Ding, W. PM_{2.5} induces Nrf2-mediated defense mechanisms against oxidative stress by activating PIK3/AKT signaling pathway in human lung alveolar epithelial A549 cells. *Cell Biol. Toxicol.* **2013**, *29*, 143–157. [[CrossRef](#)]
43. Duong, C.; Seow, H.J.; Bozinovski, S.; Crack, P.J.; Anderson, G.P.; Vlahos, R. Glutathione peroxidase-1 protects against cigarette smoke-induced lung inflammation in mice. *Am. J. Physiol.-Lung Cell. Mol. Physiol.* **2010**, *299*, L425–L433. [[CrossRef](#)]
44. Schmittgen, T.D.; Livak, K.J. Analyzing real-time PCR data by the comparative CT method. *Nat. Protoc.* **2008**, *3*, 1101–1108. [[CrossRef](#)] [[PubMed](#)]
45. Ludbrook, J. Update: Microcomputer statistics packages. A personal view. *Clin. Exp. Pharmacol. Physiol.* **1997**, *24*, 294–296. [[CrossRef](#)] [[PubMed](#)]
46. Lee, S.; Lee, D.K. What is the proper way to apply the multiple comparison test? *Korean J. Anesthesiol.* **2018**, *71*, 353–360. [[CrossRef](#)]
47. Sauder, D.C.; DeMars, C.E. An updated recommendation for multiple comparisons. *Adv. Methods Pract. Psychol. Sci.* **2019**, *2*, 26–44. [[CrossRef](#)]
48. Piper, S.L.; Laron, D.; Manzano, G.; Pattnaik, T.; Liu, X.; Kim, H.T.; Feeley, B.T. A comparison of lidocaine, ropivacaine and dexmethasone toxicity on bovine tenocytes in culture. *J. Bone Jt. Surg. Br.* **2012**, *94*, 856–862. [[CrossRef](#)] [[PubMed](#)]
49. Ku, S.K.; Kim, J.W.; Cho, H.R.; Kim, K.Y.; Min, Y.H.; Park, J.H.; Kim, J.S.; Park, J.H.; Seo, B.I.; Roh, S.S. Effect of β -glucan originated from *Aureobasidium pullulans* on asthma induced by ovalbumin in mouse. *Arch. Pharm. Res.* **2012**, *35*, 1073–1081. [[CrossRef](#)]
50. Fox, J.G.; Cohen, B.J.; Loew, F.M. *Laboratory Animal Medicine*; Academic Press. Inc.: Orlando, FL, USA, 1984.
51. Tajima, Y. *Biological Reference Data Book on Experimental Animals*; Soft Science Inc.: Tokyo, Japan, 1989.
52. Sodikoff, C.H. *Laboratory Profiles of Small Animal Diseases, A Guide to Laboratory Diagnosis*; Mosby: St. Louise, MO, USA, 1995; pp. 1–36.
53. Tumes, D.J.; Cormie, J.; Calvert, M.G.; Stewart, K.; Nassenstein, C.; Braun, A.; Foster, P.S.; Dent, L.A. Strain-dependent resistance to allergen-induced lung pathophysiology in mice correlates with rate of apoptosis of lung-derived eosinophils. *J. Leukoc. Biol.* **2007**, *81*, 1362–1373. [[CrossRef](#)]
54. Okada, S.; Kita, H.; George, T.J.; Gleich, G.J.; Leiferman, K.M. Migration of eosinophils through basement membrane components in vitro: Role of matrix metalloproteinase-9. *Am. J. Respir. Cell Mol. Biol.* **1997**, *17*, 519–528. [[CrossRef](#)]
55. Tillie-Leblond, I.; Gosset, P.; Le Berre, R.; Janin, A.; Prangère, T.; Tonnel, A.B.; Guery, B.P. Keratinocyte growth factor improves alterations of lung permeability and bronchial epithelium in allergic rats. *Eur. Respir. J.* **2007**, *30*, 31–39. [[CrossRef](#)]
56. Na, H.G.; Kim, Y.D.; Choi, Y.S.; Bae, C.H.; Song, S.Y. Diesel exhaust particles elevate MUC5AC and MUC5B expression via the TLR4-mediated activation of ERK1/2, p38 MAPK, and NF- κ B signaling pathways in human airway epithelial cells. *Biochem. Biophys. Res. Commun.* **2019**, *512*, 53–59. [[CrossRef](#)]
57. Wang, J.; Li, Y.; Zhao, P.; Tian, Y.; Liu, X.; He, H.; Jia, R.; Oliver, B.G.; Li, J. Exposure to air pollution exacerbates inflammation in rats with preexisting COPD. *Mediators Inflamm.* **2020**, *2020*, 4260204. [[CrossRef](#)] [[PubMed](#)]
58. Rose, M.C.; Nickola, T.J.; Voynow, J.A. Airway mucus obstruction: Mucin glycoproteins, MUC gene regulation and goblet cell hyperplasia. *Am. J. Respir. Cell Mol. Biol.* **2001**, *25*, 533–537. [[CrossRef](#)]
59. Groneberg, D.A.; Eynott, P.R.; Oates, T.; Lim, S.; Wu, R.; Carlstedt, I.; Nicholson, A.G.; Chung, K.F. Expression of MUC5AC and MUC5B mucins in normal and cystic fibrosis lung. *Respir. Med.* **2002**, *96*, 81–86. [[CrossRef](#)] [[PubMed](#)]
60. Henke, M.O.; Renner, A.; Huber, R.M.; Seeds, M.C.; Rubin, B.K. MUC5AC and MUC5B mucins are decreased in cystic fibrosis airway secretions. *Am. J. Respir. Cell Mol. Biol.* **2004**, *31*, 86–91. [[CrossRef](#)] [[PubMed](#)]
61. Kim, D.H.; Chu, H.S.; Lee, J.Y.; Hwang, S.J.; Lee, S.H.; Lee, H.M. Up-regulation of MUC5AC and MUC5B mucin genes in chronic rhinosinusitis. *Arch. Otolaryngol. Head Neck Surg.* **2004**, *30*, 747–752. [[CrossRef](#)] [[PubMed](#)]
62. Ballard, S.T.; Spadafora, D. Fluid secretion by submucosal glands of the tracheobronchial airways. *Respir. Physiol. Neurobiol.* **2007**, *159*, 271–277. [[CrossRef](#)] [[PubMed](#)]
63. Ueki, I.; German, V.F.; Nadel, J.A. Micropipette measurement of airway submucosal gland secretion. Autonomic effects. *Am. Rev. Respir. Dis.* **1980**, *121*, 351–357.
64. Haxhiu, M.A.; Haxhiu-Poskurica, B.; Moracic, V.; Carlo, W.A.; Martin, R.J. Reflex and chemical responses of trachea; submucosal glands in piglets. *Respir. Physiol.* **1990**, *82*, 267–278. [[CrossRef](#)]
65. Trout, L.; Corboz, M.R.; Ballard, S.T. Mechanism of substance P-induced liquid secretion across porcine bronchial epithelium. *Am. J. Physiol.* **2001**, *281*, L639–L645.
66. Phillips, J.E.; Hey, J.A.; Corboz, M.R. Tachykinin NK₃ and NK₁ receptor activation elicits secretion from porcine airway submucosal glands. *Br. J. Pharmacol.* **2003**, *138*, 254–260. [[CrossRef](#)]
67. Matsumoto, K.; Hosoya, T.; Tashima, K.; Namiki, T.; Murayama, T.; Horie, S. Distribution of transient receptor potential vanilloid 1 channel expressing nerve fibers in mouse rectal and colonic enteric nervous system: Relationship to peptidergic and nitrenergic neurons. *Neuroscience* **2011**, *172*, 518–534. [[CrossRef](#)] [[PubMed](#)]
68. Liu, H.; Fan, X.; Wang, N.; Zhang, Y.; Yu, J. Exacerbating effects of PM_{2.5} in OVA-sensitized and challenged mice and the expression of TRPA1 and TRPV1 proteins in lungs. *J. Asthma* **2017**, *54*, 807–817. [[CrossRef](#)] [[PubMed](#)]
69. Ji, Z.; Wang, Z.; Chen, Z.; Jin, H.; Chen, C.; Chai, S.; Lv, H.; Yang, L.; Hu, Y.; Dong, R.; et al. Melatonin attenuates chronic cough mediated by oxidative stress via transient receptor potential melastatin-2 in guinea pigs exposed to particulate matter 2.5. *Physiol. Res.* **2018**, *67*, 293–305. [[CrossRef](#)] [[PubMed](#)]

70. Fan, R.; Ren, Q.; Zhou, T.; Shang, L.; Ma, M.; Wang, B.; Xiao, C. Determination of endogenous substance change in PM_{2.5}-induced rat plasma and lung samples by UPLC-MS/MS method to identify potential markers for lung impairment. *Environ. Sci. Pollut. Res. Int.* **2019**, *26*, 22040–22050. [[CrossRef](#)] [[PubMed](#)]
71. Weldy, C.S.; Luttrell, I.P.; White, C.C.; Morgan-Stevenson, V.; Cox, D.P.; Carosino, C.M.; Larson, T.V.; Stewart, J.A.; Kaufman, J.D.; Kim, F.; et al. Glutathione (GSH) and the GSH synthesis gene *Gclm* modulate plasma redox and vascular responses to acute diesel exhaust inhalation in mice. *Inhal. Toxicol.* **2013**, *25*, 444–454. [[CrossRef](#)] [[PubMed](#)]
72. Jin, Y.; Wu, W.; Zhang, W.; Zhao, Y.; Wu, Y.; Ge, G.; Ba, Y.; Guo, Q.; Gao, T.; Chi, X.; et al. Involvement of EGF receptor signaling and NLRP12 inflammasome in fine particulate matter-induced lung inflammation in mice. *Environ. Toxicol.* **2017**, *32*, 1121–1134. [[CrossRef](#)] [[PubMed](#)]
73. Park, S.K.; Kang, J.Y.; Kim, J.M.; Kim, H.J.; Heo, H.J. *Ecklonia cava* attenuates PM_{2.5}-induced cognitive decline through mitochondrial activation and anti-inflammatory effect. *Mar. Drugs* **2021**, *19*, 131. [[CrossRef](#)] [[PubMed](#)]
74. Videla, L.A. Energy metabolism, thyroid calorigenesis, and oxidative stress: Functional and cytotoxic consequences. *Redox. Rep.* **2000**, *5*, 265–275. [[CrossRef](#)]
75. Subudhi, U.; Das, K.; Paital, B.; Bhanja, S.; Chainy, G.B. Alleviation of enhanced oxidative stress and oxygen consumption of L-thyroxine induced hyperthyroid rat liver mitochondria by vitamin E and curcumin. *Chem. Biol. Interact.* **2008**, *173*, 105–114. [[CrossRef](#)]
76. Venditti, P.; Di Meo, S. Thyroid hormone-induced oxidative stress. *Cell Mol. Life Sci.* **2006**, *63*, 414–434. [[CrossRef](#)]
77. Messarah, M.; Boumendjel, A.; Chouabia, A.; Klibet, F.; Abdennour, C.; Boulakoud, M.S.; Feki, A.E. Influence of thyroid dysfunction on liver lipid peroxidation and antioxidant status in experimental rats. *Exp. Toxicol. Pathol.* **2010**, *62*, 301–310. [[CrossRef](#)] [[PubMed](#)]
78. Das, K.; Chainy, G.B. Modulation of rat liver mitochondrial antioxidant defence system by thyroid hormone. *Biochim. Biophys. Acta* **2001**, *1537*, 1–13. [[CrossRef](#)] [[PubMed](#)]
79. Odabasoglu, F.; Cakir, A.; Suleyman, H.; Aslan, A.; Bayir, Y.; Halici, M.; Kazaz, C. Gastroprotective and antioxidant effects of usnic acid on indomethacin-induced gastric ulcer in rats. *J. Ethnopharmacol.* **2006**, *103*, 59–65. [[CrossRef](#)] [[PubMed](#)]
80. Cheeseman, K.H.; Slater, T.F. An introduction to free radical biochemistry. *Br. Med. Bull.* **1993**, *49*, 481–493. [[CrossRef](#)] [[PubMed](#)]
81. Ribbons, K.A.; Thompson, J.H.; Liu, X.; Pennline, K.; Clark, D.A.; Miller, M.J. Anti-inflammatory properties of interleukin-10 administration in hapten-induced colitis. *Eur. J. Pharmacol.* **1997**, *323*, 245–254. [[CrossRef](#)] [[PubMed](#)]
82. Carini, M.; Aldini, G.; Piccone, M.; Facino, R.M. Fluorescent probes as markers of oxidative stress in keratinocyte cell lines following UVB exposure. *Farmaco* **2000**, *55*, 526–534. [[CrossRef](#)] [[PubMed](#)]
83. Zaki, M.H.; Man, S.M.; Vogel, P.; Lamkanfi, M.; Kanneganti, T.D. Salmonella exploits NLRP12-dependent innate immune signaling to suppress host defenses during infection. *Proc. Natl. Acad. Sci. USA* **2014**, *111*, 385–390. [[CrossRef](#)]
84. Ryter, S.W.; Alam, J.; Choi, A.M. Heme oxygenase-1/carbon monoxide: From basic science to therapeutic applications. *Physiol. Rev.* **2006**, *86*, 583–650. [[CrossRef](#)]
85. Dong, Y.L.; Kabir, S.M.; Lee, E.S.; Son, D.S. CXCR2-driven ovarian cancer progression involves upregulation of proinflammatory chemokines by potentiating NF- κ B activation via EGFR-transactivated Akt signaling. *PLoS ONE* **2013**, *8*, e83789. [[CrossRef](#)]
86. Zheng, H.; Ying, H.; Yan, H.; Kimmelman, A.C.; Hiller, D.J.; Chen, A.J.; Perry, S.R.; Tonon, G.; Chu, G.C.; Ding, Z.; et al. p53 and Pten control neural and glioma stem/progenitor cell renewal and differentiation. *Nature* **2008**, *455*, 1129–1133. [[CrossRef](#)]
87. Qi, Q.; Ling, Y.; Zhu, M.; Zhou, L.; Wan, M.; Bao, Y.; Liu, Y. Promoter region methylation and loss of protein expression of PTEN and significance in cervical cancer. *Biomed. Rep.* **2014**, *2*, 653–658. [[CrossRef](#)] [[PubMed](#)]
88. Li, Z.H.; Li, L.; Kang, L.P.; Wang, Y. MicroRNA-92a promotes tumor growth and suppresses immune function through activation of MAPK/ERK signaling pathway by inhibiting PTEN in mice bearing U14 cervical cancer. *Cancer Med.* **2018**, *7*, 3118–3131. [[CrossRef](#)]
89. Jiang, X.; Li, H. Overexpression of LRIG1 regulates PTEN via MAPK/MEK signaling pathway in esophageal squamous cell carcinoma. *Exp. Ther. Med.* **2016**, *12*, 2045–2052. [[CrossRef](#)] [[PubMed](#)]
90. Ebbesen, S.H.; Scaltriti, M.; Bialucha, C.U.; Morse, N.; Kasthuber, E.R.; Wen, H.Y.; Dow, L.E.; Baselga, J.; Lowe, S.W. Pten loss promotes MAPK pathway dependency in HER2/neu breast carcinomas. *Proc. Natl. Acad. Sci. USA* **2016**, *113*, 3030–3035. [[CrossRef](#)] [[PubMed](#)]
91. Chen, S.; Li, D.; Zhang, H.; Yu, D.; Chen, R.; Zhang, B.; Tan, Y.; Niu, Y.; Duan, H.; Mai, B.; et al. The development of a cell-based model for the assessment of carcinogenic potential upon long-term PM_{2.5} exposure. *Environ. Int.* **2019**, *131*, 104943. [[CrossRef](#)] [[PubMed](#)]
92. Chao, X.; Yi, L.; Lan, L.L.; Wei, H.Y.; Wei, D. Long-term PM_{2.5} exposure increases the risk of non-small cell lung cancer (NSCLC) progression by enhancing interleukin-17a (IL-17a)-regulated proliferation and metastasis. *Aging* **2020**, *12*, 11579–11602. [[CrossRef](#)] [[PubMed](#)]
93. Jin, X.J.; Kim, E.J.; Oh, I.K.; Kim, Y.K.; Park, C.H.; Chung, J.H. Prevention of UV-induced skin damages by 11,14,17-eicosatrienoic acid in hairless mice in vivo. *J. Korean Med. Sci.* **2010**, *25*, 930–937. [[CrossRef](#)] [[PubMed](#)]
94. Kahari, V.M.; Saarialho-Kere, U. Matrix metalloproteinases in skin. *Exp. Dermatol.* **1997**, *6*, 199–213. [[CrossRef](#)]
95. Woessner, J.F., Jr. Role of matrix proteases in processing enamel proteins. *Connect. Tissue Res.* **1998**, *39*, 69–73. [[CrossRef](#)]
96. Nagase, H.; Woessne, J.F., Jr. Matrix metalloproteinases. *J. Biol. Chem.* **1999**, *274*, 21491–21494. [[CrossRef](#)]
97. Sternlicht, M.D.; Werb, Z. How matrix metalloproteinases regulate cell behavior. *Annu. Rev. Cell Dev. Biol.* **2001**, *17*, 463–516. [[CrossRef](#)] [[PubMed](#)]
98. Yang, B.; Guo, J.; Xiao, C. Effect of PM_{2.5} environmental pollution on rat lung. *Environ. Sci. Pollut. Res. Int.* **2018**, *25*, 36136–36146. [[CrossRef](#)] [[PubMed](#)]

99. Jiang, Y.; Zhao, Y.; Wang, Q.; Chen, H.; Zhou, X. Fine particulate matter exposure promotes M2 macrophage polarization through inhibiting histone deacetylase 2 in the pathogenesis of chronic obstructive pulmonary disease. *Ann. Transl. Med.* **2020**, *8*, 1303. [[CrossRef](#)] [[PubMed](#)]
100. Monian, P.; Jiang, X. Clearing the final hurdles to mitochondrial apoptosis: Regulation post cytochrome C release. *Exp. Oncol.* **2012**, *34*, 185–191. [[PubMed](#)]
101. Wang, A.S.; Xu, Y.; Zhang, Z.W.; Lu, B.B.; Yin, X.; Yao, A.J.; Han, L.Y.; Zou, Z.Q.; Li, Z.; Zhang, X.H. Sulforaphane protects MLE-12 lung epithelial cells against oxidative damage caused by ambient air particulate matter. *Food Funct.* **2017**, *8*, 4555–4562. [[CrossRef](#)] [[PubMed](#)]
102. Li, X.; Ding, Z.; Zhang, C.; Zhang, X.; Meng, Q.; Wu, S.; Wang, S.; Yin, L.; Pu, Y.; Chen, R. MicroRNA-1228(*) inhibit apoptosis in A549 cells exposed to fine particulate matter. *Environ. Sci. Pollut. Res. Int.* **2016**, *23*, 10103–10113. [[CrossRef](#)] [[PubMed](#)]
103. Xiong, S.; Mu, T.; Wang, G.; Jiang, X. Mitochondria-mediated apoptosis in mammals. *Protein Cell.* **2014**, *5*, 737–749. [[CrossRef](#)] [[PubMed](#)]
104. Choi, H.Y.; Jung, T.Y.; Ku, S.K.; Yang, H.B.; Lee, H.S. Toxicopathological study of p,p-DDE after experimental aerosol exposed to ICR Mouse. *Toxicol. Res.* **2005**, *21*, 151–160.
105. Honda, H.; Fujimoto, M.; Miyamoto, S.; Ishikawa, N.; Serada, S.; Hattori, N.; Nomura, S.; Kohno, N.; Yokoyama, A.; Naka, T. Sputum Leucine-rich alpha-2 glycoprotein as a marker of airway inflammation in asthma. *PLoS ONE* **2016**, *11*, e0162672. [[CrossRef](#)]
106. Hu, J.R.; Jung, C.J.; Ku, S.M.; Jung, D.H.; Ku, S.K.; Choi, J.S. Antitussive, expectorant, and anti-inflammatory effects of Adenophorae Radix powder in ICR mice. *J. Ethnopharmacol.* **2019**, *239*, 111915. [[CrossRef](#)]
107. Wang, D.; Wang, S.; Chen, X.; Xu, X.; Zhu, J.; Nie, L.; Long, X. Antitussive, expectorant and anti-inflammatory activities of four alkaloids isolated from Bulbus of *Fritillaria wabuensis*. *J. Ethnopharmacol.* **2012**, *139*, 189–193. [[CrossRef](#)]
108. Negara, B.F.S.P.; Kim, J.W.; Bashir, K.M.I.; Lee, J.H.; Ku, M.U.; Kim, K.Y.; Shin, S.; Hong, E.-J.; Ku, S.K.; Choi, J.-S. Expectorant effects of immature Asian pear extract on PM_{2.5}-induced subacute pulmonary injury in mice. *J. Food Biochem.* **2023**, *2023*, 5671679. [[CrossRef](#)]
109. Kim, M.R.; Bashir, K.M.I.; Lee, J.H.; Ku, M.U.; Kim, J.W.; Kim, K.Y.; Shin, S.; Hong, E.-J.; Ku, S.K.; Choi, J.-S. Efficacy confirm test of immature Asian pear extracts on the ovalbumin-induced asthma in mice. *Appl. Sci.* **2023**, *13*, 9342. [[CrossRef](#)]

Disclaimer/Publisher's Note: The statements, opinions and data contained in all publications are solely those of the individual author(s) and contributor(s) and not of MDPI and/or the editor(s). MDPI and/or the editor(s) disclaim responsibility for any injury to people or property resulting from any ideas, methods, instructions or products referred to in the content.